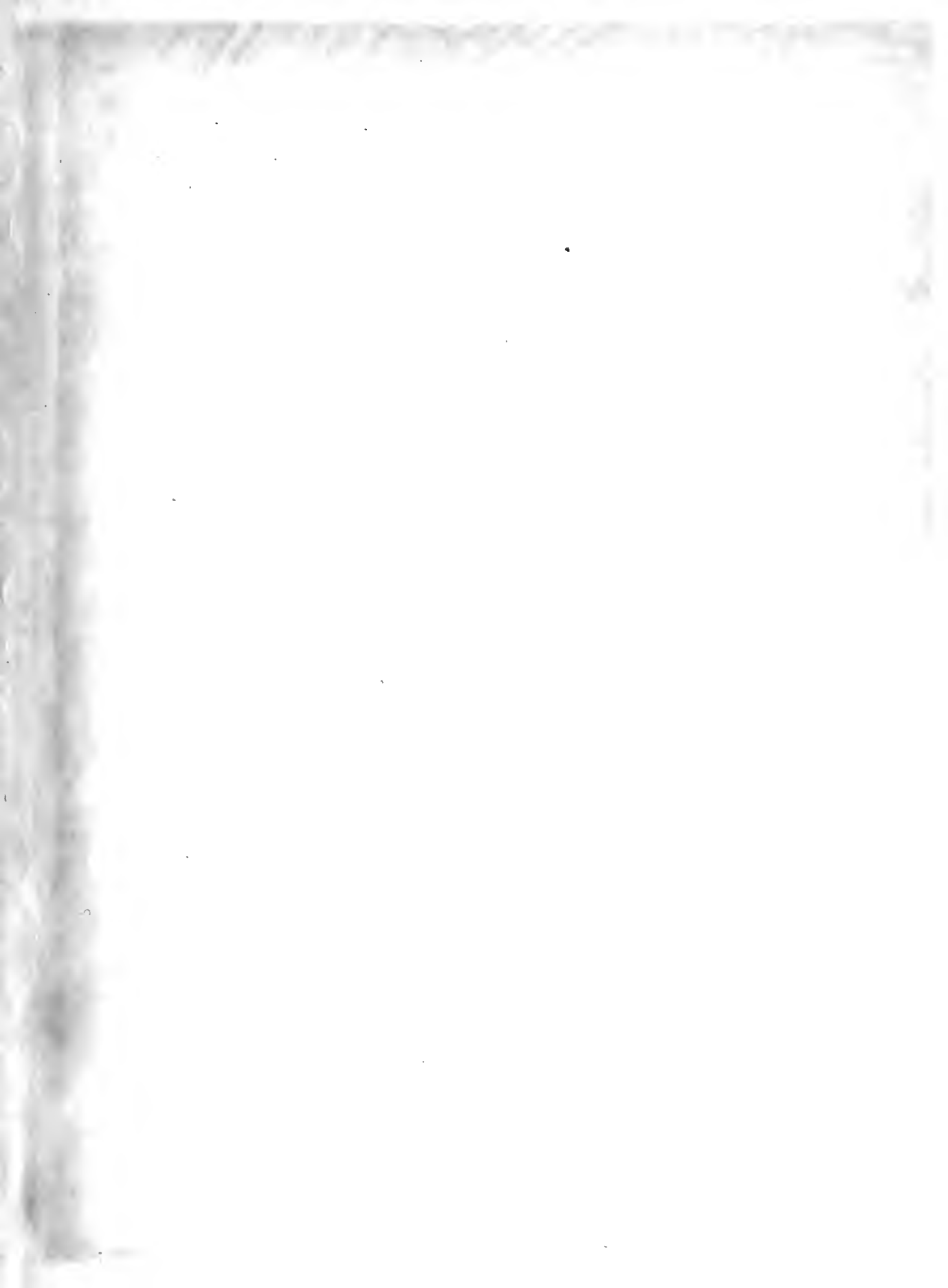


**A DRIFT FREE GAMMA RAY SPECTROMETER  
FOR NEUTRON RADIOACTIVATION ANALYSIS**

---

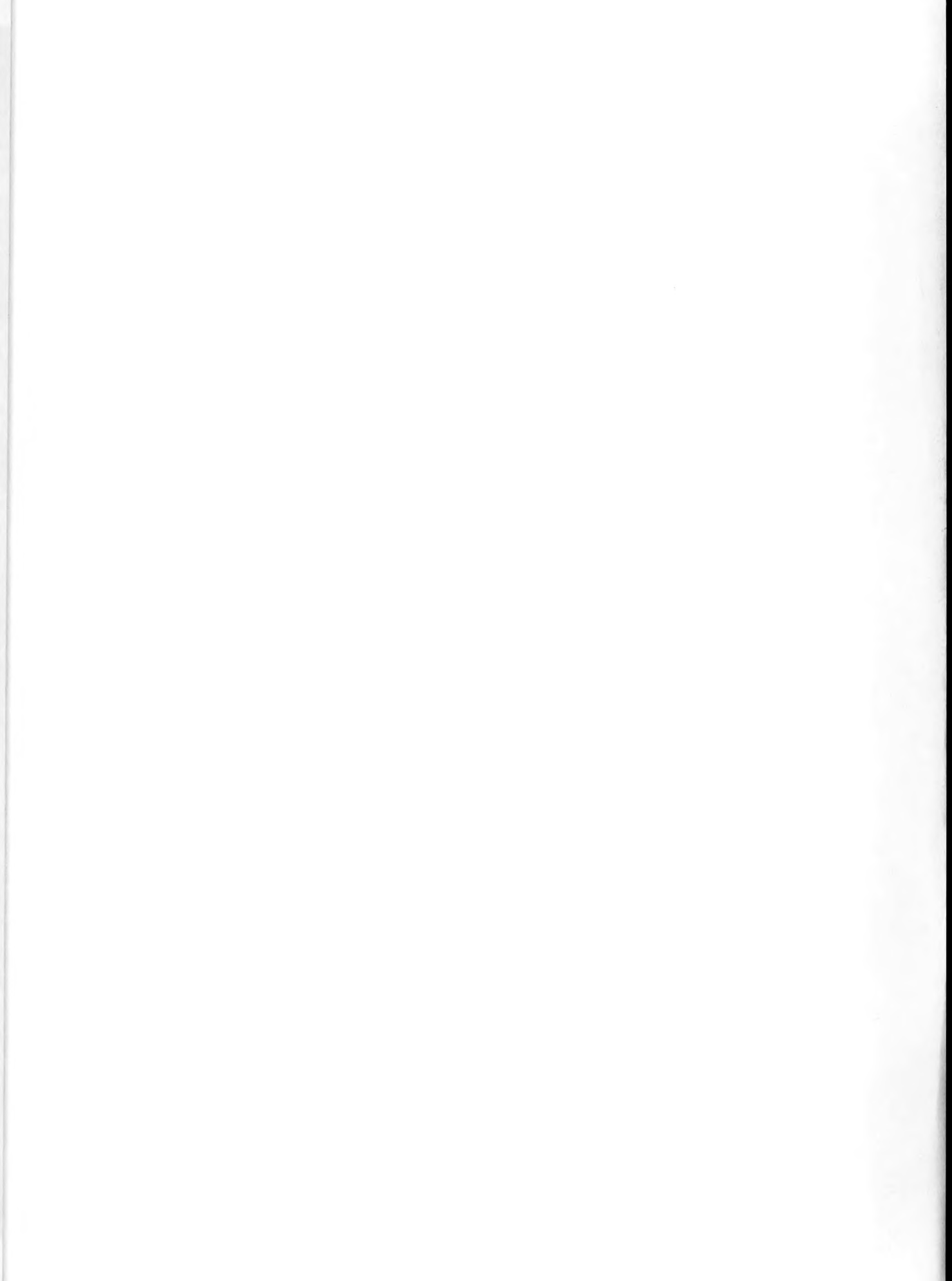
**Ernest Brenton Altekruze**

LIBRARY  
U.S. NAVAL POSTGRADUATE SCHOOL  
MONTEREY, CALIFORNIA









A DRIFT FREE GAMMA RAY SPECTROMETER  
FOR  
NEUTRON RADIOACTIVATION ANALYSIS

\*\*\*\*\*

Ernest B. Altekruze





8854

ALTEKRUSE

1956

THESIS  
A425

Letter on cover:

A DRIFT FREE GAMMA RAY  
SPECTROMETER FOR NEUTRON  
RADIOACTIVATION ANALYSIS

Ernest Brenton Altekkruse



A DRIFT FREE GAMMA RAY SPECTROMETER  
FOR NEUTRON RADIOACTIVATION ANALYSIS

by

Ernest Brenton Altekruze

Captain, United States Marine Corps

Submitted in partial fulfillment  
of the requirements  
for the degree of  
MASTER OF SCIENCE  
IN  
ENGINEERING ELECTRONICS

United States Naval Postgraduate School  
Monterey, California

1 9 5 6

Thesis  
A425

This work is accepted as fulfilling  
the thesis requirements for the degree of

MASTER OF SCIENCE  
IN  
ENGINEERING ELECTRONICS

from the  
United States Naval Postgraduate School



## PREFACE

The work presented in this paper was accomplished during an eleven week industrial tour with the Engineering Physics and Analysis Laboratory of the General Electric Company, Schenectady, New York.

The General Electric Company is one of many industrial concerns which has recognized the value of the neutron radioactivation method of analysis and is striving to broaden the applications of the method. Cognizant of the desirability of an extremely sensitive and accurate analytical technique, the Engineering Physics and Analysis Laboratory decided to embark upon a project of development of a drift free gamma ray spectrometer.

It is the aim of the writer to present in this paper the general methods of neutron radioactivation analysis, one system of instrumentation used in activation analysis, and the development of the desired drift free gamma ray spectrometer from that system.

The writer wishes to express his gratitude to the staff of the Engineering Physics and Analysis Laboratory for making available the equipment and the time necessary for the completion of the project and for their advice and assistance during the project.





# TABLE OF CONTENTS

Item	Title	Page
Chapter I	Introduction . . . . .	1
Chapter II	Method of Neutron Activation Analysis for Gamma-Ray Spectroscopy . . . . .	4
Chapter III	Advantages, Limitations and Applications of Neutron Activation Analysis for Gamma-Ray Spectroscopy . . . . .	14
Chapter IV	Instrumentation for Neutron Activation Analysis, the Gamma-Ray Spectrometer . . . . .	17
Chapter V	Drift in the Gamma-Ray Spectrometer . . . . .	48
Chapter VI	Elimination of Drift in the Gamma-Ray Spectrometer . . . . .	52
Chapter VII	Conclusions . . . . .	71
Bibliography	. . . . .	72
Appendix I	Table of Sensitivity Comparisons . . . . .	74
Appendix II	Chart of Nuclides . . . . .	77



# LIST OF ILLUSTRATIONS AND TABLES

Figure	Page
1. Block diagram of a gamma ray spectrometer . . . . .	18
2. Sketch of NaI(Tl) crystal and container . . . . .	22
3. Gamma ray spectrum, component effects and combined effects .	25
4. Spectrogram of Co <sup>60</sup> and Cs <sup>137</sup> samples . . . . .	28
5. Schematic diagram of photomultiplier tube (DuMont 6364) . . .	31
6. Photograph of DuMont 6364 multiplier phototube (half size). .	32
7. Oscillograph of Co <sup>60</sup> and Cs <sup>137</sup> spectra . . . . .	45
8. Photograph of main portion of spectrometer, including amplifier, pulse height analyzer, linear count rate meter, recorder and oscilloscope . . . . .	47
9. Drift characteristics of spectrometer before correction . . .	51
10. Drift characteristics of spectrometer after modification . .	68
11. Block diagram of modified gamma ray spectrometer . . . . .	70
12. Schematic diagram of design preamplifier for use with gamma ray spectrometer . . . . .	63
13. Plot of drift characteristics of multiplier phototube with operation at various high voltages . . . . .	87
14. Circuit diagram of gamma ray spectrometer . . . . .	88
15. Chart of Nuclides . . . . .	86

## Table

1. Tabulation of data for the determination of drift in the gamma ray spectrometer . . . . .	50
2. Tabulation of data for the determination of drift after modification of the gamma ray spectrometer . . . . .	67
3. Sensitivity comparisons . . . . .	74



# TABLE OF SYMBOLS AND ABBREVIATIONS

(Listed in order of their appearance in the text)

$n, n^1$	neutron, a neutral elemental particle of mass number one
$\gamma, \gamma^0$	gamma ray, a quantum of electromagnetic radiation emitted by a nucleus, each such photon being emitted as the result of a quantum transition between two energy levels of the nucleus. Zero charge and zero mass
X	nucleus of bombarded atom in general reaction equations
A	atomic mass number, the mass of a neutral atom of a nuclide, usually expressed in terms of the atomic mass unit which is 1/16th the mass of a neutral atom of the most abundant isotope of oxygen, $O^{16}$ . Also used to denote activity
Z	atomic number; the positive charge of the nucleus in multiples of the electronic charge, e, also the number of protons in the nucleus
Q	disintegration energy, the energy evolved, or the negative of the energy absorbed, in a nuclear disintegration
$P, p^1$	proton, an elemental particle of mass number one and one associated positive charge
$\alpha, \alpha^4$	alpha particle, a positively charged particle, of mass number four and positive charge two, composed of two protons and two neutrons, identical in all measured properties with the nucleus of a helium atom
Y	nucleus of isotopic product of a nuclear reaction, in general equations
$\beta, \beta^-, \beta^+$	beta ray or beta particle, $\beta^-$ , a negative electron or, $\beta^+$ , a positive electron emitted from a nucleus during decay
ev	electron volt, unit of energy, equal to energy gained by a particle having one electronic charge when it passes in a vacuum through a potential difference of one volt. One ev = $1.6 \times 10^{-12}$ ergs



Mev	million electron volts, one Mev = $10^6$ ev
$\sigma$	cross section, a measure of the probability of occurrence of a given reaction, the effective area of the nucleus for the reaction expressed in barns, where one barn = $10^{-24}$ square centimeters
$N^*$	number of radioactive nuclei present in sample at time of consideration
t	time, measured after start of irradiation for activating elements in sample. $t = 0$ at start of irradiation
f	neutron flux, for irradiation, measured in neutrons/square centimeter second
N	number of parent nuclei present in sample at time of consideration
$\lambda$	radioactive decay constant, the probability per unit time that a given unstable particle or system, such as a radioactive atom, will undergo spontaneous transformation
T	half life, the time required for the decay of one-half the atoms of a sample of a radioactive substance
ln	natural logarithm operator, the natural logarithm of a number is the index of the power to which the base e must be raised in order to equal the number
C	constant of integration
e	napierian base, $e = 2.7182818$
$\tau$	time, measured after removal of activated sample from flux, $\tau = 0$ at instant of removal from flux
$N_t^*$	number of radioactive nuclei present at the end of irradiation
A	activity of radioisotope anytime during irradiation process, measured in disintegrations/unit time
$A_t$	activity of radioisotope at the end of the irradiation process
$A_\tau$	activity of radioisotope anytime after irradiation has ceased





dx	incremental distance in direction of x axis within a crystal
dB	incremental change of beam intensity, as beam travels a distance dx in the crystal
B	intensity of gamma ray beam at any depth x in crystal
B <sub>0</sub>	intensity of beam incident upon surface of crystal
$\mu$	linear absorption coefficient, fractional decrease in intensity of gamma ray beam per unit distance traversed in crystal
$\text{\AA}$	Angstrom unit, a unit of length, $1\text{\AA} = 10^{-10}$ meters
E	energy of a gamma ray, the particular quantum of electromagnetic energy in electron volts
$\nu$	frequency of the electromagnetic radiation, units are per second
h	Planck's constant, $h = 6.624 \times 10^{-34}$ joule-seconds
m	symbol for mass
c	velocity of light in a vacuum, $c = 3 \times 10^8$ meters/second
$\mu\mu\text{fd}$	micromicrofarad, $10^{-12}$ farads, when one farad is that capacitance which maintains an electrical potential difference of one volt between two conductors charged with equal and opposite electrical quantities of one coulomb
db	decibel, the difference in two intensities $I_1$ and $I_2$ respectively expressed in decibels is $\phi$ , where $\phi = \log_{10} \frac{I_2}{I_1}$
k	one thousand
$i_{th}$	current component due to thermionic emission, measured in amperes
G	gain of the multiplier phototube
$K_1$	constant of proportionality
n	number of dynode stages in multiplier phototube



R	secondary emission ratio, ratio of number of secondary electrons emitted from a dynode surface to number of primary electrons striking dynode surface
V	interstage voltage, potential difference between two consecutive dynode stages
$K_2$	another constant of proportionality
$V_0$	overall voltage, potential difference between first and last dynode stages



## CHAPTER I

### INTRODUCTION

The past century has seen the development of many methods for analyzing the composition of materials. One of these methods, possessing a number of desirable characteristics is neutron radio-activation analysis. The discovery of artificial radioactivity in 1933 [10] laid the ground work for this new system of analysis. The system utilizes the fact that most elements, when placed in a neutron flux, form radioactive products which have their own individual radiation spectrum and decay characteristics. These characteristics act, in a way, like finger prints, and can be used to identify the parent element. The first application of the method to a complicated analytical problem was by Hevesy and Levi in 1936 [8], when they detected the presence of small amounts of rare earths present in a specimen.

The method of activation analysis was hampered during its early stages, by the unavailability of satisfactory sources of neutron flux for irradiating samples. The coming of the nuclear reactor, with its intense neutron flux, gave real impetus to the method.

Once activated, an element can be detected by numerous methods varying in sensitivity. These include photographic emulsions, ionization chambers such as Geiger Mueller counters and proportional counters and scintillation counters such as the gamma ray spectrometer. The method of detection utilized depends largely upon the purpose which dictates the analysis. For the detection of radioactivity,



photographic emulsions can be used. However, if quantitative measurements are desired, carefully controlled conditions are required when using photographic emulsions. Even then the ionizing effects of the radiation must be determined by the degree of blackening of a photographic plate, giving questionable results at best. Gamma ray scintillation spectroscopy, on the other hand, can be used to detect trace elements of the order of  $10^{-12}$  grams under ideal conditions. This characteristic of extreme sensitivity, coupled with the increasing availability of neutron flux sources for research work has led to a wide spread acceptance of gamma ray spectroscopy as a valuable analytical tool.

The electronic circuitry used in the gamma ray spectrometer is another variable depending largely upon the type of measurements desired. For instance, if the problem is to detect the presence of one specified impurity in a given bulk material, the circuitry and the whole procedure is much simpler than if the problem is to tell what unknown impurities are present in a sample and in what amounts.

For the present project it was desired to set up a system of instrumentation, using for the most part commercially available component units which could be used to demonstrate the feasibility of analyzing biological specimens, especially human tissue and body fluids. Because of the numerous trace elements present in such specimens and the proximity of their many energy peaks in the gamma ray spectrum, it was desired to develop a relatively drift free gamma ray spectrometer. With such a spectrometer one could be sure that an observed





gamma ray energy peak was truly the peak associated with the detected energy level and not an adjacent peak which had drifted to a wrong position on the chart.

The project will be presented in three phases in this paper:

- a) the general methodology of neutron activation analysis,
- b) a description of the instrumentation employed for gamma ray spectroscopy and
- c) the development of the desired drift free gamma ray spectrometer.



## CHAPTER II

### METHOD OF NEUTRON ACTIVATION ANALYSIS FOR GAMMA RAY SPECTROSCOPY

The general method of neutron activation analysis will be covered to furnish a knowledge of the type of signal being measured by the spectrometer and how that signal is obtained.

A nucleus is a combination of neutrons and protons. There is a certain probability that this combination of neutrons and protons may transform into another combination. If this probability is great, the nucleus is said to be unstable or radioactive. A radioactive nucleus will decay to form a new nucleus combination which may also be unstable. Finally a state will be reached which is stable and the activity will have ceased.

A flux of nuclear particles falling on a nucleus of an atom may cause that nucleus in some way to change and become unstable. The nuclear particle flux used in activation may be derived from one of the following sources:

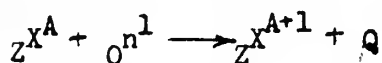
- (a) Nuclear reactor (neutrons),
- (b) Cyclotron (protons, deuterons, alpha particles, neutrons),
- (c) Betatron (gamma rays, neutrons),
- (d) Linear accelerator (protons, neutrons, deuterons) [16] and
- (e) Particle accelerators of the Van de Graff type (electrons, protons, alpha particles, neutrons).

For the most part, analysts choose the neutron as the nuclear particle with which to bombard the nucleus.



During this project two irradiation procedures were used exclusively. The samples were either sent to Brookhaven National Laboratory where they could be placed in a reactor with a maximum flux of thermal, or slow neutrons<sup>(1)</sup> of  $4 \times 10^{12}$  neutrons/cm<sup>2</sup>-sec or of fast neutrons<sup>(2)</sup> of  $4 \times 10^{11}$  neutrons/cm<sup>2</sup>-sec; or they were irradiated using the General Engineering Laboratory linear accelerator, having a maximum flux of fast neutrons of  $2 \times 10^7$  neutrons/cm<sup>2</sup>-sec. Using a water moderator to slow down the neutrons it was possible to obtain thermal neutrons from the accelerator.

With neutron activation there are four primary interactions. The first and most important is the neutron-gamma/ray, (n, $\gamma$ ), reaction which occurs most frequently when the flux is of thermal neutrons. Here the nucleus, X, of an atom of the irradiated sample captures a slow neutron. The mass number, A, of the nucleus is increased by one unit while the atomic number, Z, does not change. The reaction is written



where Q is the disintegration energy, appearing mainly as gamma ray energy, which can be detected.

Since the (n, $\gamma$ ) reaction is the most important to the analyst, it is worthwhile to examine several actual reactions of this type<sup>(3)</sup>.

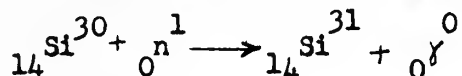
First let us look at the reaction which takes place when Cadmium 113,  ${}_{48}^{113}\text{Cd}$ , is bombarded by thermal neutrons

- (1) Thermal or slow neutrons have an energy of approximately 0.025 ev or lower.
- (2) Fast neutrons are those having energies greater than 1000 ev, 14.5 Mev from the linear accelerator.
- (3) See any standard chemistry textbook for list of elements, their abbreviations, atomic numbers and atomic mass numbers.

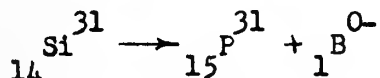




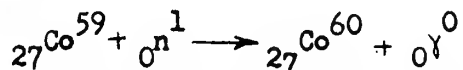
The gamma ray which appears here is not the one detected in the method of gamma ray spectroscopy. This gamma ray is called the "capture" gamma ray and is the one emitted during the (n,γ) nuclear reaction. In this particular reaction the product  ${}_{48}^{114}\text{Cd}$  is not radioactive. Thus, thermal neutron activation is not applicable for detecting the presence of  ${}_{48}^{113}\text{Cd}$  by gamma ray spectroscopy. When Silicon 30,  ${}_{14}^{30}\text{Si}$ , is placed in a thermal neutron flux the reaction is



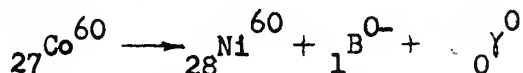
the  ${}_{14}^{31}\text{Si}$  does decay by emitting a beta particle



giving Phosphorous 31. The decay is not accompanied by the emission of gamma rays, the method does not detect beta particles, so, again the method is not applicable to the particular reaction. A large number of (n,γ) reactions have radioactive products which do emit gamma rays as they decay. It is in these cases that the methods of gamma ray spectroscopy have their application. Cobalt 59,  ${}_{27}^{59}\text{Co}$ , reacts with thermal neutrons as follows



in which  ${}_{27}^{60}\text{Co}$  is radioactive. The  ${}_{27}^{60}\text{Co}$  decays forming Nickel 60,  ${}_{28}^{60}\text{Ni}$

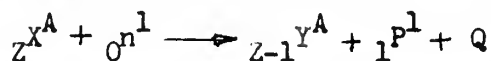


The beta particle goes undetected, however the gamma ray is detected by the spectrometer.

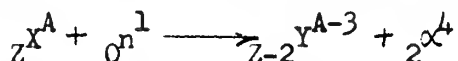




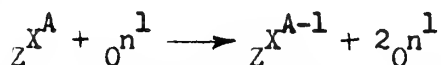
With faster neutrons the  $(n,\gamma)$  reaction is somewhat suppressed and other interactions show up with significant abundance. These include the neutron-proton,  $(n,p)$ , neutron-alpha,  $(n,\alpha)$ , and the neutron-two neutron,  $(n,2n)$ , reactions. In the  $(n,p)$  reaction the mass number remains the same while the atomic number decreases by one, by the addition of a neutron and subtraction of a proton



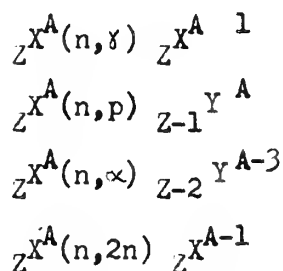
Y being a new element nucleus since the atomic number has changed. For the  $(n,\alpha)$  reaction, the addition of a neutron and subtraction of an alpha particle lowers the atomic number of the nucleus by two and the mass number by three. This reaction can be written



Finally there is the  $(n,2n)$  reaction in which the capture of one neutron by the nucleus causes the emission of two neutrons. Here the atomic number remains constant while the mass number decreases by one, which can be expressed



These four reactions are often cited in the literature and the notation shortened to



where the nucleus on the left is the target nucleus, the nucleus on the right is the product nucleus, the particle on the left inside the



parenthesis is the bombarding particle, and the particle on the right within the parenthesis is the emitted particle. The products of nuclear reactions produced by neutron bombardment can be determined by recourse to the literature. The results are available in tabular [13] and chart (see Appendix II) form.

The nuclear reactions will proceed with a certain efficiency depending upon the target nucleus and the energy of the neutrons in the flux. That is, for every atom there is a certain probability that a neutron of a given energy will be captured by the nucleus of that atom. This probability has the units of square centimeters and is called the cross section,  $\sigma$ , for the reaction. Cross section values are tabulated in the literature [9,11,12]. A typical cross section for neutron activation of an individual nucleus is of the order of  $10^{-24} \text{ cm}^2$  and for convenience this has been called one barn. As suggested before, the most efficient reaction for thermal neutrons is the  $(n,\gamma)$ , in most cases the occurrence of the other reactions,  $(n,p)$ ,  $(n,\alpha)$ , and  $(n,2n)$  at this level is negligible. However, as the neutron energy is increased the cross sections for the other reactions usually increase, while that for the  $(n,\gamma)$  decreases. The most efficient overall reaction is the  $(n,\gamma)$  reaction at low neutron energy levels. Other factors such as neutron resonances of certain nuclei, may necessitate activation with higher energy neutrons. The cross section values as listed in the literature presently available are very complete for thermal neutron reactions while not nearly so complete for fast neutrons. This is another feature which dictates the use of thermal neutron activation for analysis work.



Besides the cross section which is determined by the parent atom and the neutron energy, the intensity of the radiation depends upon the following:

- (a) the flux density,
- (b) the number of parent isotopes available (as used in the text, the number of parent isotopes includes the factors of elemental concentration and isotopic abundance),
- (c) the time of exposure of the sample to the flux and
- (d) the rate of decay of the activated nuclei.

The relationships by which the activity may be computed will be developed mathematically. The rate of growth,  $\frac{dN^*}{dt}$ , of the number of radioactive nuclei is given by

$$\frac{dN^*}{dt} = \sigma f N - \lambda N^* \quad (1) \quad [3]$$

where  $\sigma f N$  is the production factor, depending upon the cross section for the reaction,  $\sigma$ , the flux density,  $f$ , and the number of parent nuclei,  $N$ , present at any time.  $\lambda N^*$  is the rate of decay of radioactive nuclei.

Nuclei which have become active during bombardment will decay as the bombardment progresses. The rate of decay is proportional to the number of active nuclei,  $N^*$ , present. The constant of proportionality,  $\lambda$ , is called the radioactive decay constant and is given by the formula

$$\lambda = \frac{0.693}{T} \quad (2) \quad [3]$$

where  $T$  is the half life of the radioactive product. Production and decay will proceed until an equilibrium point is reached. At this point the particular element is fully activated and further irradiation will produce no gain in activity.

The growth rate equation can be rearranged and integrated directly



$$\frac{dN^*}{\frac{\sigma f N}{\lambda} - N^*} = \lambda dt$$

$$-\ln\left(\frac{\sigma f N}{\lambda} - N^*\right) = \lambda t + C$$

At  $t = 0$ , the start of irradiation, the number of radioactive nuclei is zero, that is  $N^* = 0$ . Applying this boundary condition the constant of integration,  $C$ , is evaluated

$$-\ln\left(\frac{\sigma f N}{\lambda}\right) = C$$

then

$$\lambda t = -\ln\left(\frac{\sigma f N}{\lambda} - N^*\right) + \ln\left(\frac{\sigma f N}{\lambda}\right)$$

$$= -\ln\left(1 - \frac{N^*}{\frac{\sigma f N}{\lambda}}\right)$$

$$e^{-\lambda t} = \left(1 - \frac{\lambda N^*}{\sigma f N}\right)$$

$$\frac{\lambda N^*}{\sigma f N} = 1 - e^{-\lambda t}$$

and

$$N^* = \frac{\sigma f N}{\lambda} (1 - e^{-\lambda t}) = \frac{\sigma f N}{\lambda} \left(1 - e^{-\frac{0.693t}{T}}\right) \quad (3)$$

Thus, the function which follows the growth of the radioactive nuclei during irradiation is an exponential function. Equation (3) will enable the analyst to compute the number of radioactive nuclei present at the instant of completion of irradiation, however, he is usually concerned with measuring the activity at some time later, say when the sample has been removed from the flux and placed in a detection system.

Once removed from the flux, the production factor of the growth rate equation is eliminated and there is only negative growth or decay.





$$\frac{dN^*}{d\tau} = -\lambda N^* \quad (4)$$

where  $\tau$  is used to designate time after removal from the flux. Integrating

$$\begin{aligned} \frac{dN^*}{N^*} &= -\lambda d\tau \\ \ln N^* &= -\lambda\tau + C \end{aligned}$$

at  $\tau = 0$ , the completion of irradiation,  $N^* = N_t^*$  and

$$C = \ln N_t^*$$

so

$$\ln N^* = -\lambda\tau + \ln N_t^*$$

$$\ln\left(\frac{N^*}{N_t^*}\right) = -\lambda\tau$$

$$N^* = N_t^* e^{-\lambda\tau} \quad (5)$$

exhibiting an exponential decay.

We now have a method for computing the number of radioactive nuclei present at any time during the irradiation - decay process. The activity,  $A$ , at any time, is proportional to the number of radioactive atoms by the radioactive decay constant,  $\lambda$ , and is measured in disintegrations per unit time

$$A = \lambda N^* \quad (6) \quad [3]$$

thus, at the end of irradiation

$$A_t = \lambda N_t^* = \sigma f N (1 - e^{-\lambda t}) = \sigma f N (1 - e^{-\frac{0.693t}{T}}) \quad (7)$$

and at any time  $\tau$  after that

$$A_\tau = A_t e^{-\lambda\tau} = A_t e^{-\frac{0.693\tau}{T}} \quad (8)$$

By using equation (8) and counting the number of disintegrations per unit time at two different times after irradiation, it is possible to compute the half life of the element. The radioactivity that existed at



the end of bombardment can also be computed if the time that has elapsed since the sample was taken from the flux is known. Further, the number of parent atoms present at the start of irradiation may be calculated if the period of irradiation has been recorded, provided the element has by now been identified. The identity of the element is required to furnish the cross section value for the activation process.

The half life gives one of the identifying characteristics of the parent element. The association may be made by reference to tables [20] or a nuclide chart (see Appendix II). To attempt to identify accurately on this basis alone would not prove satisfactory since many activated nuclei have nearly equal half lives. Fortunately when a radioisotope disintegrates it emits radiations which are also characteristic of the isotope and this offers another clue as to the identity of the parent element. The most significant radiations which may be emitted during decay are

- (a) Alpha particles,  $\alpha$ ,
- (b) Negatrons,  ${}_1\text{B}^{0-}$ ,
- (c) Positrons,  ${}_1\text{B}^0$ , and
- (d) Gamma rays.

In the spectroscopic procedures related to this project, the reaction involving gamma rays is of prime concern. Numerous characteristics of the other types of radiation make them undesirable for the purpose. These include low penetrating powers and random energy distributions. On the other hand a very desirable aspect of gamma ray spectroscopy lies in the mono-energetic nature of gamma ray radiation. Each active nuclei which emits gamma rays does so at discrete energy levels. During



its decay, a nucleus may give off a single gamma ray at one specific level or several gamma rays, each at a discrete energy level. For example, two radioactive specimens were used as standards during this project; cobalt-60, ( $\text{Co}^{60}$ ), with two associated gamma ray energies, one at 1.172 Mev and the other at 1.332 Mev and cesium-137, ( $\text{Cs}^{137}$ ), with a single gamma ray energy of 0.663 Mev. With each radioactive nucleus having its peculiar gamma radiation spectrum, another means of identification is available.

As mentioned before, with the element once identified it is possible to compute accurately the number of atoms of the parent isotope present in the original sample. However, performing the mathematical computations of such a method can become laborious and, in practical application, a simpler procedure of comparison with a standard is employed. Since the identity of the element present in the sample is now known we may irradiate a carefully weighed amount of the same element, the standard, under conditions identical with the irradiation of the sample. In this way, a standard is produced. Then, observing the activities of the sample and the standard at comparable times, the weight of the element in the sample is given by

$$\frac{\text{weight of element in sample}}{\text{weight of standard}} = \frac{\text{activity of element in sample}}{\text{activity of standard}} \quad (9) \quad [15]$$

Thus by examining the gamma ray spectrum of a sample, an analysis as to the identity and the quantity of elements present in the sample can be obtained.



CHAPTER III  
ADVANTAGES, LIMITATIONS AND APPLICATIONS  
OF NEUTRON ACTIVATION ANALYSIS  
FOR GAMMA RAY SPECTROSCOPY

The most obvious advantage derived in using neutron activation as an analytical method is its extreme sensitivity under favorable conditions. Meinke [15] has compared activation analysis with five other typical trace analysis methods (see Appendix I) and the comparison is favorable for the former. Another factor is the unique set of radiation energies and decay characteristics possessed by the activated nuclei. Thus, the method, when applicable is more direct and positive than other analytical procedures.

Consideration of contamination during analysis is another major advantage. A minimum handling prior to irradiation is possible, since the introduction of the sample in its original form into the irradiation flux is all that is required. After irradiation the danger of contamination is essentially eliminated since all elements in the sample are now activated while subsequent contaminants most likely are not radioactive and, thus, will not show up in the detection process. Except for the radiation hazards to the analyst, this means that the sample after irradiation is much easier to work with than in other analytical methods.

There are, of course, limitations inherent in activation analysis, as with any other method. Since we have chosen gamma ray detection there is an obvious weakness in the method; some activated nuclei do not emit gamma rays. If this is the situation, another method must be





utilized, as, for example, beta ray spectroscopy or direct current arc spectrographic analysis methods.

Radioactive nuclei with very short half lives may become highly active very quickly and die away to insignificant, sometimes undetectable, activities with equal rapidity. At times nearly complete decay may occur before any detection procedures can be inaugurated. On the other hand, activated nuclei with very long half lives, having low cross sections, may not produce sufficient activity to be detected in reasonable irradiation times.

The method often is hampered by the bulk material activity overriding the trace element activity in a given sample. Since the bulk material is normally known and the trace element is that which it is desired to determine, this is undesirable. In this case, the procedure yielding maximum sensitivity must be determined and carried out. For example, if the bulk material is composed of elements having low cross section and long half lives, while the trace elements have short half lives and high cross sections, the sample may be irradiated for a short period and quickly analyzed. In this manner the trace elements are detected at near full activity while the bulk activity is as yet insignificant. Conversely, if the bulk is of short half life with high cross section and the trace of long half life and low cross section, the sample may be irradiated for a long period. All constituents will rise to high activity, then analysis is delayed until the activity of the bulk material dies off. In unfavorable circumstances the bulk and trace element half lives and cross sections may be nearly equal. In this case the sample can be



irradiated and the constituents chemically separated, without worry as to what contaminants have been added in the separation process.

It is to be understood that atoms can be detected as individual elements but no information is obtained concerning their structural positions within compounds. However, knowing the percentage composition of a sample may give a clue as to what compounds are present.

At the present time the applications of the method are quite wide and the outlook for the future is for further broadening. A few applications are the determination of trace elements in alloys and metals, drugs, fertilizers, food, fuels, glass, lubricants, minerals, ores, paints, plastics, soils, and water. To point out a few specific applications more familiar to the writer the following are mentioned:

- (a) detection of trace elements in jet aircraft fuel,
- (b) determination of impurities in germanium for transistor production,
- (c) detection of pollution of river water and
- (d) studies of the trace element content of biological specimens.

It was in regard to the last mentioned area that the present project was proposed. There are studies now in progress [17] which concern the analysis of cancerous and non-cancerous tissue as to trace element content. The belief is that a thorough study along these lines may give the medical profession new insight into variations in biochemical composition of neoplastic tissue. Activation analysis and gamma ray spectroscopy seem well adapted for making this study [18] in view of the nature of the trace elements which may be present.



CHAPTER IV  
INSTRUMENTATION FOR NEUTRON ACTIVATION ANALYSIS  
THE GAMMA RAY SPECTROMETER

It has been pointed out that accurate measurement of the emitted gamma ray energies and the activity decay characteristics furnishes data valuable to the computation of the composition of a sample. The arrangement of the gamma ray radiations of a sample as to energy level and frequency of occurrence is called its gamma ray spectrum. The system of instrumentation for observing this spectrum is called a gamma ray spectrometer. The principle involved is that of a scintillation counter.

For the spectrometer to do its job adequately it must:

- (a) convert the gamma ray energy into an electric pulse of amplitude proportional to that gamma ray energy,
- (b) separate the signals as to pulse amplitudes,
- (c) count the signal pulses in the separate levels and
- (d) present the results to the analyst in the desired form.

A general instrumentation system which will accomplish this is shown in block diagram in Figure 1. The individual components utilized in the instrumentation will be explained in detail in the remainder of this chapter.

#### 1. CRYSTAL

When gamma rays pass through matter they interact with the atoms which make up that matter. Gamma rays, because of their electromagnetic nature, may lose energy by interactions with electrons or nuclei. Certain liquids and crystals have the property of giving off visual scintillations



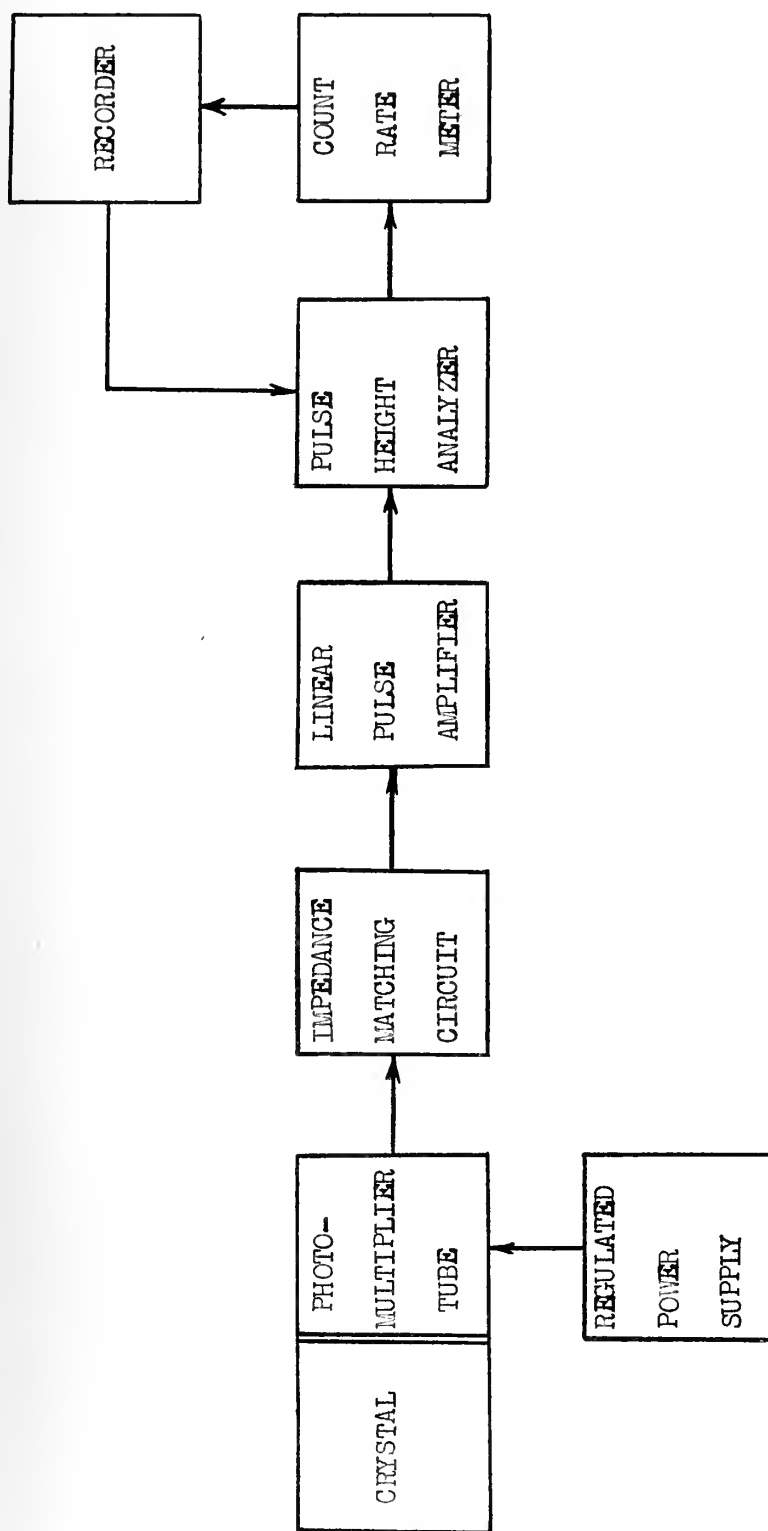


Figure 1. Block diagram of a gamma ray spectrometer





when gamma rays pass through them.

Phosphor crystals such as anthracene and Stilbene, which are organic crystals, and Calcium tungstate, ( $\text{CaWO}_4$ ), and sodium iodide activated with thallium,  $\text{NaI}(\text{Tl})$ , which are inorganic, are often used to absorb gamma ray energy. These crystals will absorb incident gamma rays and convert their electromagnetic energy into flashes of light. The intensity of these flashes under favorable conditions, will be proportional to the energy given up by the gamma rays. The choice of a particular crystal depends largely upon its phosphor fluorescent efficiency, light collection efficiency, cost, and certain other physical qualities.

The phosphor fluorescent efficiency of a crystal is based upon its ability to stop gamma rays and upon the number of light photons emitted for a given gamma ray energy absorbed. When a beam of gamma rays falls upon a crystal the intensity of the beam decreases with depth of penetration, much as the intensity of a sunbeam decreases in passing through a cloud or smoke. As the beam travels a distance,  $dx$ , through the crystal it loses intensity by the amount  $-dB$  where  $B$  is the intensity of the beam at any depth,  $B_0$  is the incident intensity and  $\mu$  is the absorption coefficient of the crystal material.

$$dB = -\mu B \, dx \quad (10) \quad [19]$$

integrating

$$\frac{dB}{B} = -\mu dx$$

$$\ln B = -\mu x + C$$



evaluation of C, when  $x = 0$  and  $B = B_0$

$$\ln B_0 = C$$

gives

$$\ln \frac{B}{B_0} = -\mu x$$

$$B = B_0 e^{-\mu x} \quad (11)$$

Thus, it is desirable to have a crystal with a large value of  $\mu$  so that a reasonable sized crystal may be used. On the basis of this stopping power anthracene can be eliminated as it is a poor absorber of gamma rays. Stilbene is an improvement in this respect, yet, not quite as good as the NaI(Tl) or  $\text{CaWO}_4$  crystals.

The number of photons of light emitted per Mev of gamma ray energy absorbed differs considerably for various crystals. The intensity of the light must be such that it will show above the photomultiplier tube noise. The three crystals remaining are satisfactory in this respect. Stilbene, however, yields only about a third the light intensity of the other two crystals.

Another stipulation which must be placed upon the light emitted by the crystal is that it be of such a wave length that it will stimulate the photosensitive cathode of the photomultiplier. This criterion is fulfilled by the three crystals named above [18] .

The emitted light also, must not be self absorbed within the crystal. NaI(Tl) and  $\text{CaWO}_4$  crystals emit light of wave lengths in the region of 4000 Å, and are transparent to fluorescent emissions in this same range. Of the three crystals, the  $\text{CaWO}_4$  crystal inflicts the least self absorption upon its emissions.



The growth and finishing of crystals is a complicated and expensive procedure. Stilbene is brittle, breaking easily under shock.  $\text{CaWO}_4$  is an extremely hard jewel-like crystal, not easily worked. These traits add to the difficulty of the finishing process and tend to make the expenses involved prohibitive. On the other hand,  $\text{NaI(Tl)}$  is easily cut, readily machinable and relatively inexpensive.

There are several other physical characteristics which determine the crystal selection. Stilbene oxidizes and forms a cloudy film.  $\text{NaI(Tl)}$  is deliquescent and must be protected from air and moisture.  $\text{CaWO}_4$  is a very clear crystal. However, while the other two crystals have short decay times, which allow the light from one pulse to fade away before the next occurs,  $\text{CaWO}_4$  with a relatively long decay time [18] is just inside the maximum useable value.

In light of the above considerations, a  $\text{NaI(Tl)}$  crystal was chosen for use with the spectrometer. The crystal and container were produced by the Harshaw Chemical Company and their general configuration is shown in Figure 2. The glass seal toward the tube allows the photomultiplier to see the light flashes. The magnesium oxide,  $\text{MgO}$ , coating acts as a reflector for light attempting to leave in any undesired direction, channeling all light toward the photomultiplier tube. The container was evacuated to protect the crystal from air and moisture. The well allows the sample to be placed within the crystal for more efficient gamma ray gathering and the thick aluminum around the well shields out any undesired alpha and beta radiations. The characteristics of an  $\text{NaI(Tl)}$  crystal, that is, absorption coefficient for various gamma ray energies and source



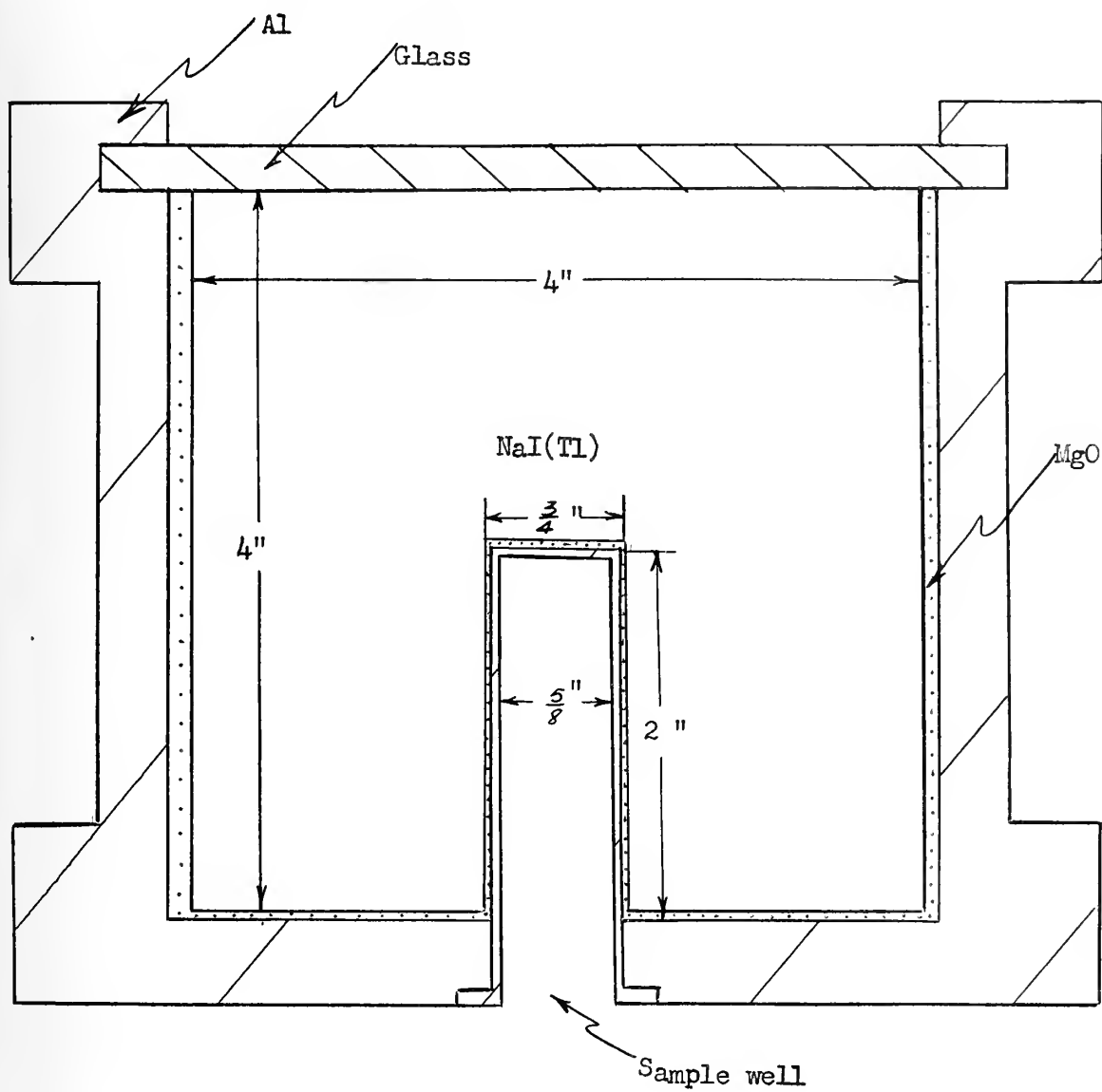


Figure 2. Sketch of NaI(Tl) crystal and container





distances, wave length of light emitted, efficiency with various energy gamma rays, decay time of light pulse, etc. are available in the literature [11] .

A gamma ray, as previously mentioned, will have a discrete amount of energy associated with it. This energy,  $E$ , which a gamma ray possesses is proportional to its frequency,  $\nu$ , the constant of proportionality,  $h$ , being Planck's constant ( $h=6.624 \times 10^{-34}$  joule-seconds).

$$E = h\nu \quad (12) \quad [7]$$

A gamma ray of discrete energy is sometimes called a quantum of electromagnetic radiation. A gamma ray may lose its associated energy in one of three basic ways. The three ways are:

- (a) photoelectric effect,
- (b) pair production and
- (c) scattering or Compton effect.

In the photoelectric effect each gamma ray gives up all its energy to an electron which is bound to a nucleus. With the energy thus gained the electron escapes its bonds. A part of the energy is dissipated during the escape process, the remainder appears as the kinetic energy of the electron. This escaped electron is called a photoelectron. The photoelectron loses its energy by collision with other electrons still associated with the phosphor crystal causing them to give off flashes of light. The flashes have an intensity proportional to the gamma ray energy absorbed. As the energy spectrum is scanned, counts of activity (peaks) are obtained only at these energy levels and the sums of these energy levels and nowhere else. The sums are included since for each



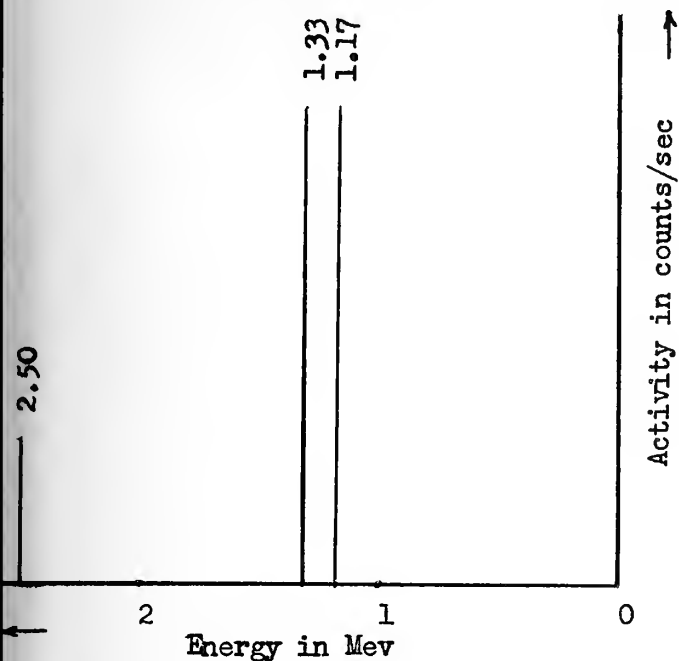
disintegration more than one energy gamma ray may be emitted and the photomultiplier may sometimes see the two or more scintillations simultaneously and not be able to differentiate between them. In this coincidence case, the spectrometer sees the two light flashes as one, with an associated energy which is the sum of the two. The peak thus obtained is called the summation peak. As an illustration, using a  $\text{Co}^{60}$  standard, with gamma ray energies of 1.17 Mev and 1.33 Mev the summation peak would appear at 2.50 Mev. Considering only the photo-electric effect the spectrum would appear as in Figure 3a.

Pair production, in which the gamma ray energy is converted into an electron and a positron, requires gamma rays of energy greater than 1 Mev. Here energy,  $E$ , is transformed into mass,  $m$ , and by Einstein's equation this requires

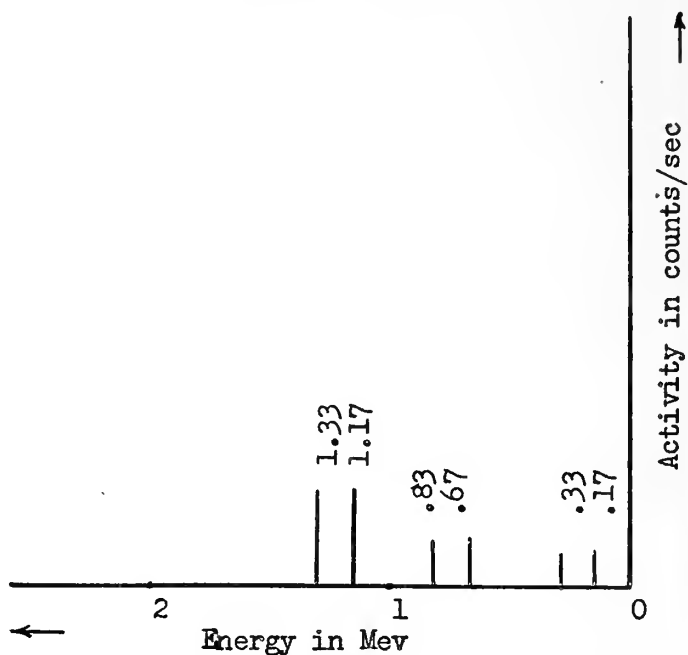
$$E = mc^2 \quad (13) \quad [7]$$

where  $c$  is the velocity of light in a vacuum ( $c = 3 \times 10^8$  meters/second). The creation of each of the masses, the positron and electron (negatron) requires approximately 0.5 Mev, therefore the combined transformation demands one Mev of energy. Any excess of energy would be divided between the electron and positron as increased kinetic energy. The kinetic energy of the electron and positron is absorbed in the usual manner. As the positron comes to rest it combines with a nearby electron resulting in the annihilation of the two mass particles and the liberation of two 0.5 Mev gamma rays. These gamma rays, in turn, may escape from the crystal or be absorbed in it. In this manner two peaks are obtained; one at 0.5 Mev, if one of the gamma rays escaped, and one at 1 Mev, if neither

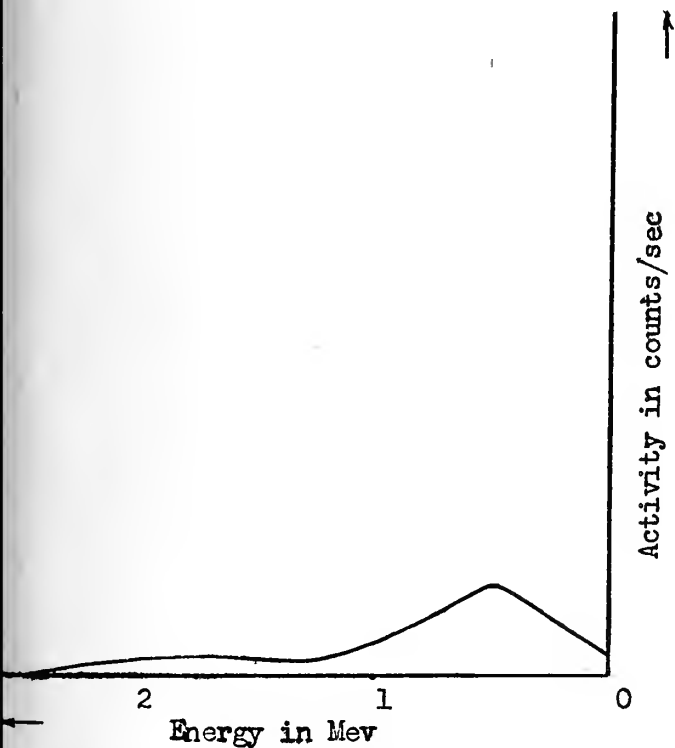




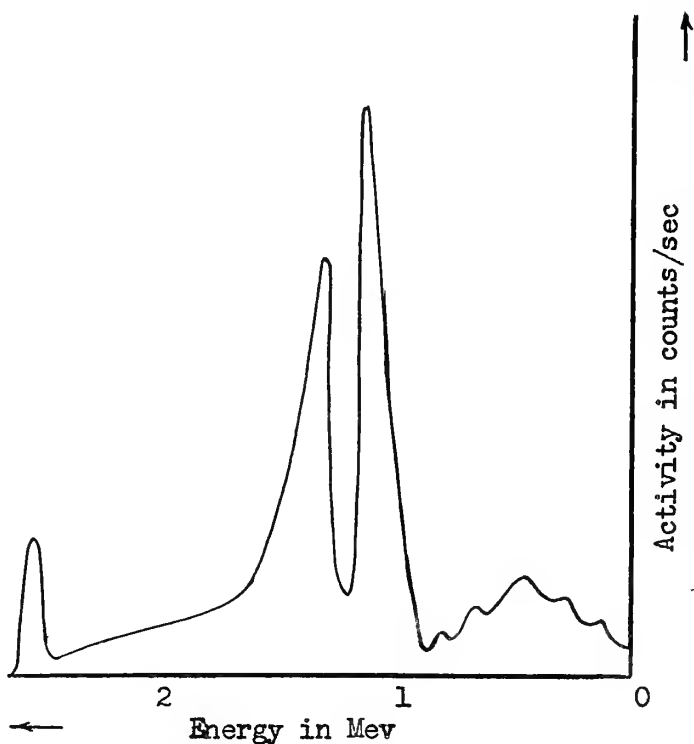
3a. Gamma ray spectrum, photoelectric effect



3b. Gamma ray spectrum, pair production



3c. Gamma ray spectrum, Compton effect



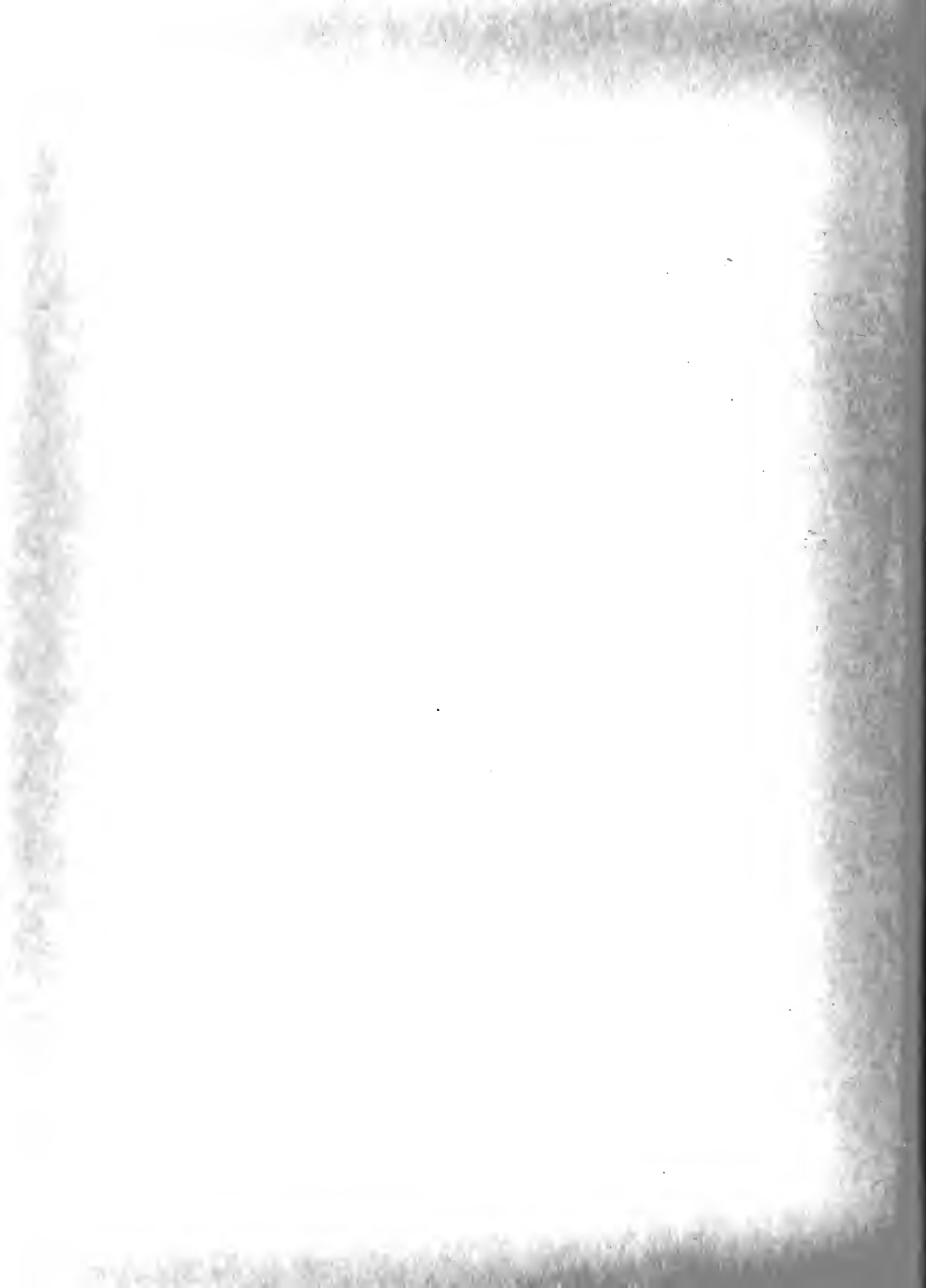
3d. Gamma ray spectrum, combined effects



escaped (provided there was no additional gamma energy which had been converted into kinetic energy). If, as is the case with  $\text{Co}^{60}$ , there is additional energy (1.17 Mev and 1.33 Mev instead of 1 Mev) the additional energy would be absorbed in stopping the electron and positron. Peaks will therefore occur at 1.33 Mev, 0.83 Mev and 0.33 Mev and 1.17 Mev, 0.67 Mev and 0.17 Mev depending upon whether neither, one or both gamma rays of 0.5 Mev escape crystal absorption. This is demonstrated in Figure 3b.

Scattering or Compton effect is a process in which gamma rays, instead of being absorbed, are diverted from their original direction by collisions with electrons. In this type interaction the total energy and momentum remains constant. An electron, which deflects a gamma ray, picks up the energy lost by the gamma ray. The gamma ray loses energy by changing frequency. The energy transferred from the gamma ray to the electron varies from nearly zero to almost the total energy possessed by the gamma ray. It is evident then that this type process will produce pulses distributed throughout the energy spectrum. Somewhere between zero and  $180^\circ$ , the angle of predominant deflections will occur. The energy loss of the gamma ray at this angle will depend on its original energy. The peak associated with this scattering angle is called the Compton peak. This condition for  $\text{Co}^{60}$  appears in Figure 3c.

Unfortunately all three of these processes occur in a given spectrum, the result appearing as in Figure 3d. The useful identifying peaks are obtained via the photoelectric effect and pair production processes. They appear above the background caused by the scattering





process.

It must be borne in mind that Figure 3 is used only as a visual aid and is not presented as entirely accurate. For instance, the peaks of the  $\text{Co}^{60}$  curve may or may not be of the same height, that is the same number of counts. The number of counts depends upon the efficiency of the crystal at the different energy levels being counted. Then too, the summation peak may not appear, or may appear with many less counts than portrayed, depending on the ability of the spectrometer in separating two near simultaneous light flashes. The Compton effect may not have a distribution exactly as shown., It is believed that the figure is of enough value in following the written explanation that it is included here.

Figure 4a is a photograph of results obtained by scanning the gamma ray spectrum of a  $\text{Co}^{60}$  sample. The photoelectric peaks and the Compton background are clearly evident in the photograph. The pulses occurring at near zero energy level can most probably be attributed to noise introduced by the various electronic components. Figure 4b is a spectrogram of  $\text{Cs}^{137}$ .  $\text{Cs}^{137}$  emits gamma rays of only one energy, that being 0.66 Mev. In Figure 4b the 0.66 Mev peak is apparent as is the Compton peak and background. Notice, too, how abruptly the spectrum drops off after the photoelectric peak, just as it did after the summation peak for  $\text{Co}^{60}$  in Figure 4a.

## 2. MULTIPLIER PHOTOTUBE

A multiplier phototube is a phototube which incorporates within it an electron multiplier. For the spectrometer a DuMont type 6364



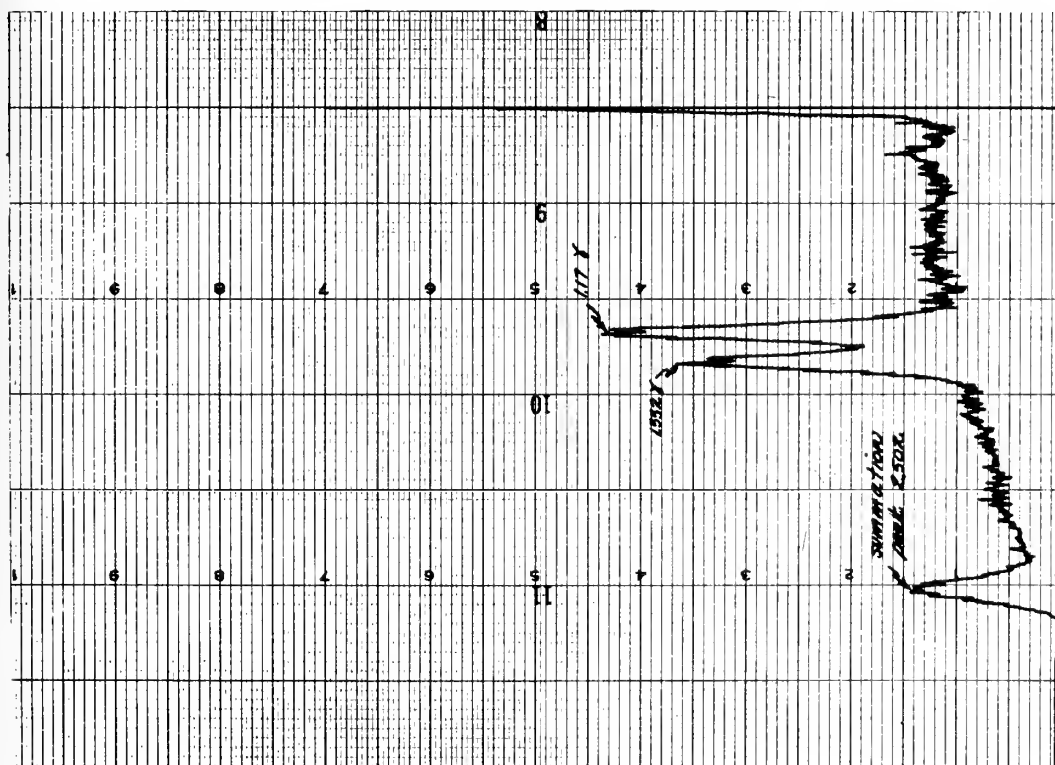


Figure 4a. Spectrogram of  $\text{Co}^{60}$

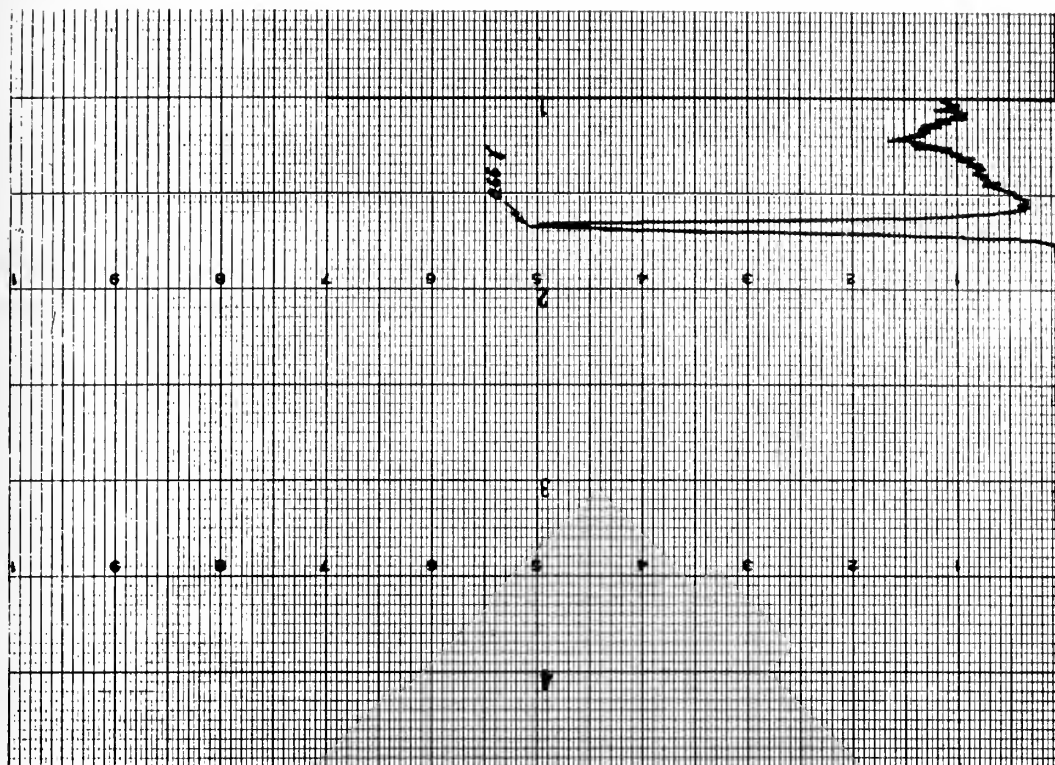
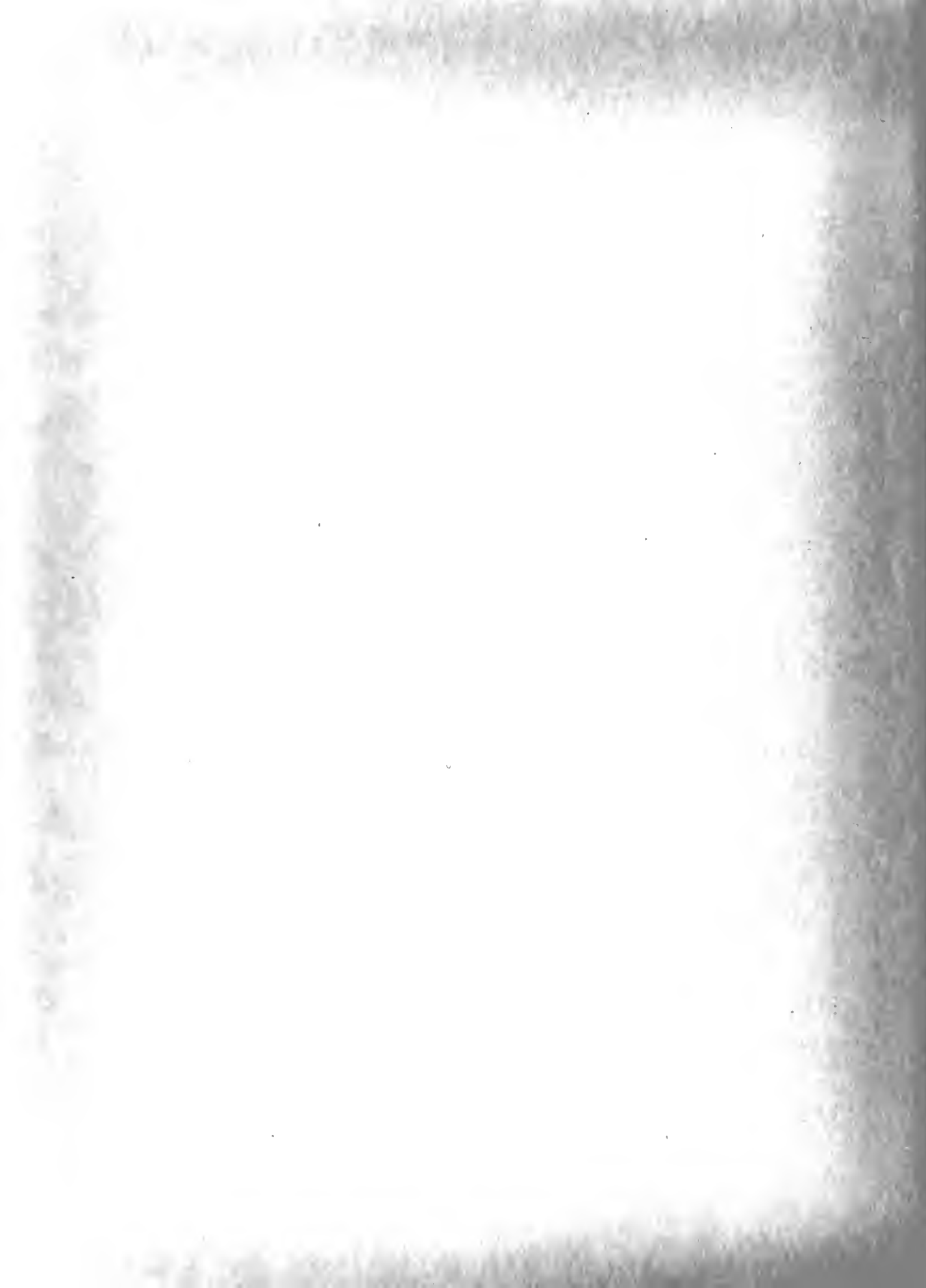


Figure 4b. Spectrogram of  $\text{Cs}^{137}$



multiplier phototube is used. This tube has a large photosensitive surface, the cesium-antimony cathode, and can be coupled to the crystal in such a manner that only one tube is needed to see the entire crystal. Actually the face of the tube is  $5\frac{1}{4}$  inches in diameter and its window is  $4\frac{3}{16}$  inches. These dimensions are too large for the tube to fit in the shallow crystal well, adjacent to the glass window of the crystal housing, which would be the ideal situation. A plexiglass plug was fashioned for the well so that the photomultiplier tube had a smooth surface to rest against. Between the photomultiplier and plexiglass surface was placed a film of fluid Silicon, Dow Corning 200 Fluid. The function could have been accomplished using smaller tubes coupled through light pipes so as to view the entire crystal. However, light pipe coupling may cause loss of resolution. A factor favoring the use of a large photomultiplier, such as the 6364, over smaller ones was the larger physical separation between anode and photocathode, tending to lower leakage currents because of the longer leakage paths in the tube. Lower leakage currents giving an improvement in signal-to-noise ratio. The location of the photocathode is also a favorable factor in the 6364. Some phototubes have the photosensitive element located centrally within the tube and their light geometry is poor. The photocathode of the 6364 is at the face of the tube and the resulting light geometry is the best possible for viewing the crystal. Uniformity of cathode sensitivity is obviously essential. Any portion of the cathode picking up a flash from the crystal must release a number of electrons proportional to the flash intensity and the factor of proportionality



must be constant over the cathode surface. A schematic diagram of the photomultiplier appears in Figure 5 and may be helpful in following the functioning of the tube. A photograph of the tube is included in Figure 6, the tube appears here half size.

The cathode pin 14, sees a low intensity light flash in the crystal and it frees a number of electrons. The number of electrons freed are proportional to the intensity of the light pulse, therefore, also proportional to the gamma ray energy causing the pulse. The liberated electrons are focused by the electrostatic field associated with the shield, pin 13, onto dynode #1. The shield has two additional functions. It shields the cathode region from the dynode electrostatic fields and protects the photocathode from positive ion bombardment. The electrons falling on dynode #1 cause secondary emission and many more electrons leave dynode #1 than impinged upon it. This amplification is repeated in each successive stage and is determined by the kinetic energy of the electrons as they strike the dynode, which in turn is controlled by the voltage between dynode stages. The overall amplification of the tube is the product of the amplifications of each stage and is of the order of  $10^5$ . The electrons emitted from the final stage, dynode #10, are collected by the anode, pin 11, and they constitute the output current of the phototube.

Individual photomultiplier tubes differ in their inherent noise and in their ability to resolve gamma ray energy peaks. (In gamma ray spectroscopy the measure of resolution is taken as the ratio of the width, measured in energy units, of a peak at half its height to the





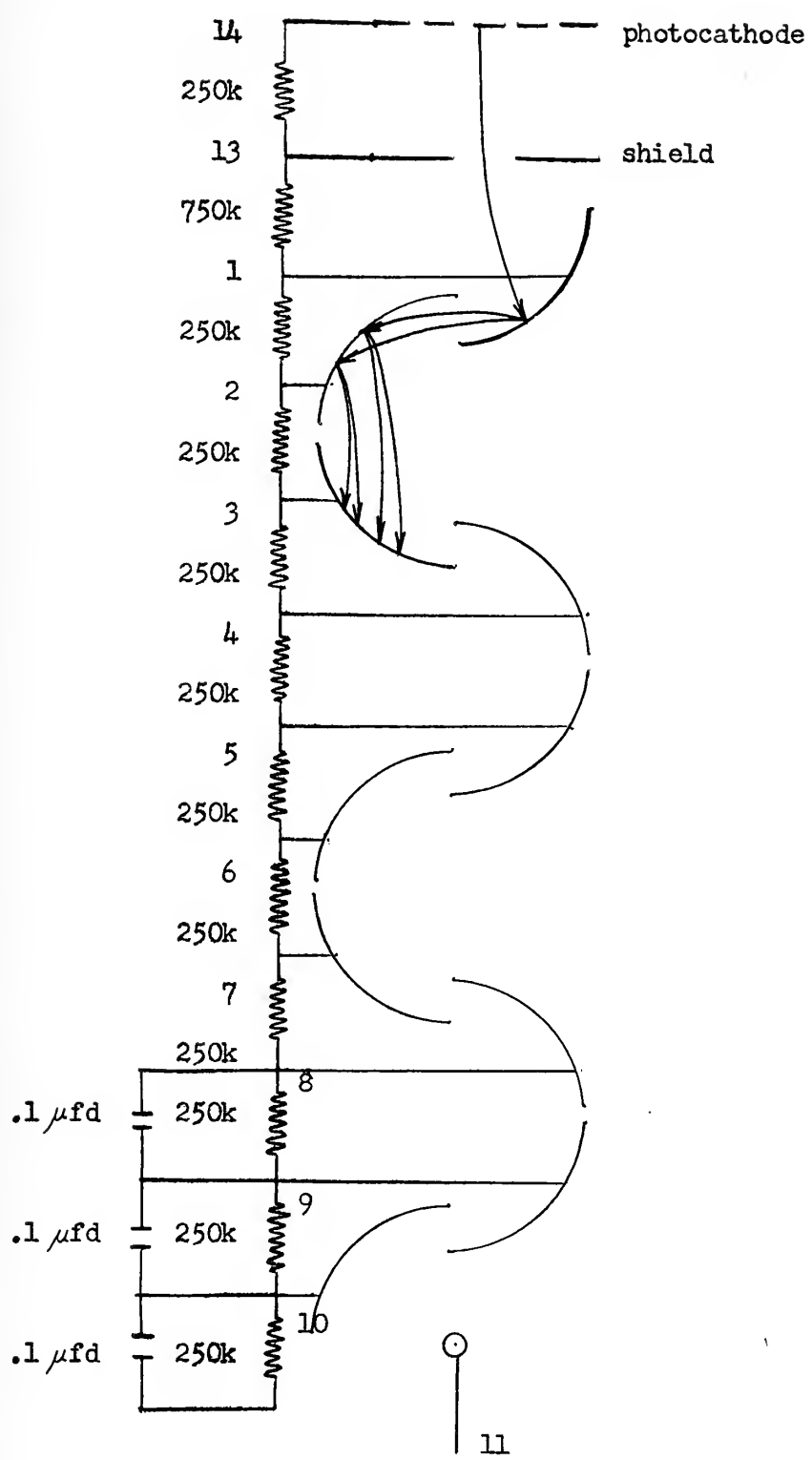


Figure 5. Schematic diagram of photomultiplier tube ( DuMont 6364 )





Figure 6. Photograph of DuMont 6364  
Multiplier Phototube (Half Size)



mean energy of the peak). For optimum sensitivity each tube should be tested for noise and resolving power before being put to use in a spectrometer.

The main causes of noise in a photomultiplier tube are thermal current and positive ion feedback current. Theoretically, the thermal noise could be eliminated by bringing the tube to  $0^{\circ}$  K which, of course, is impossible. In the present system, cooling the tube is not necessary, since the total noise of the phototube is below that of any of the other electronic components. The effects of thermal and positive ion feedback currents were not separated because of the unavailability of equipment for cooling the tube to, say  $113^{\circ}$  K. [ 4 ] The overall noise of the photomultiplier was obscured by noise from other sources while the voltage applied to the tube remained at normal values. At a level of 1700 volts on the tube, phototube noise was measurable above the noise of other electronic components at .00006 volts at the photomultiplier output terminals and continued to rise as the voltage was increased.

The resolving ability of a tube seems to be more a characteristic of the individual tube than of the voltage distribution placed on the tubes. Of three tubes tested, all were able to resolve the standard  $\text{Co}^{60}$  peaks, however, two were better than the third. The resolution of a tube is actually closely related to the noise introduced by the tube. If the background noise level is high, the sharp energy lines broaden into hump type peaks and the ability to differentiate between peaks occurring closely together is lessened. Thus a lowering of the noise level in general improves resolution. The focusing of the electron



beam, it would seem, would also affect the resolution. The focusing of the beam is largely controlled by the electrostatic fields associated with the dynodes, thus with their shape. The dynode shapes are fixed as manufactured. The only indication as to the effect of focusing on resolution is available in changing the potential upon the shield. At either extreme, that is, with the shield at cathode or dynode #1 potential, there is a definite lessening in resolution. In the recommended operating range, with shield at 10% to 40% of the potential between photocathode and dynode #1, the effect of varying shield potential upon resolution was imperceptible.

The photocathode is designed to be sensitive to light pulses of low intensity, therefore, it must be shielded from light of normal intensity. If exposed to intense light the multiplication characteristics of the tube will change temporarily. It is also desirable to shield the tube from external magnetic and electrostatic fields and to shield the crystal from undesired radioactivity. These shielding functions are accomplished by placing the tube and crystal in an aluminum light tight container and placing the whole unit in a lead brick cubicle.

The voltages which are applied to the photomultiplier are high, therefore attention should be given to the generation of noise in the tube socket. A socket constructed of mica filled phenolic is adequate for this purpose. The bleeder network used to properly distribute the voltage to the various dynodes must be chosen in light of the high voltage supply current available. Large valued resistors tend to be less stable and to contribute more noise. If lower value resistors are





used care must be taken that generated heat can be dissipated without raising the temperature of the photomultiplier tube. The bleeder network is shown in Figure 5. It is an external network connected to the pins as illustrated.

The high voltage applied to the tube should be well filtered so that noise pulses, which might be introduced through it, will not find their way to the amplifier. High voltage capacitors can be used for this purpose. The filtering requirement is especially stringent where the anode is at a high positive voltage and the cathode grounded. Conversely when the cathode is at high negative voltage and the anode grounded the need is lessened since voltage variations will affect only photomultiplier tube gain and are not as readily transmitted to the amplifier. For this reason the original instrumentation was with negative high voltage applied to the cathode.

In view of the high gain of the photomultiplier it is necessary to take precautions against the large output currents having any influence on the initial stages. This is accomplished by decoupling the last few stages with capacitors in parallel with the bleeder resistors.

The load resistor on the phototube does not determine the phototube gain; however it may limit the amplitude of the output pulse. The light flashes in the NaI(Tl) crystal have a rise time of approximately  $10^{-11}$  seconds and decay in some time of the order of 0.25 microseconds. The output current of the phototube rises in about  $10^{-9}$  seconds and decays in approximately 0.25 microseconds. This current pulse appears at the anode. The annode has a certain output capacitance shunted by the



distributed cable capacitance and the input capacitance of the next component part. Across this combined capacitance a voltage is built up. The load resistor is used to return this voltage level to zero. If the decay time for the voltage pulse is too rapid the amplitude of the pulse may be drastically reduced, if the decay time is too slow the next pulse may come along before the first has decayed. Actually, with the value of resistance chosen there is an integrating action at the phototube output terminals. This is corrected by differentiating the pulse later on in the amplifier. The time constant should be approximately two or three microseconds long in order to accommodate most amplifiers yet not require coincidence correction circuits for normal counting rates.

### 3. IMPEDANCE MATCHING CIRCUIT

A low capacitance cable of as short a length as practicable is recommended for connecting the photomultiplier to the amplifier [5] in order to lower the attenuation of the signal as much as possible. In this particular system the crystal phototube assembly could not be housed in the room which contained the rest of the spectrometer for several reasons. One reason being that the space within the room was not adequate for placing a well shielded crystal photomultiplier unit in close proximity to the rest of the spectrometer components. Another reason being that a betatron located on the same level as the main portion of the spectrometer introduced radiation which necessitated shielding in excess of that normally required. Therefore, the crystal and photomultiplier were placed in a pit one floor below the spectrometer proper and a cable and two pulse transformers were used to bring the



signal to the amplifier with minimum attenuation.

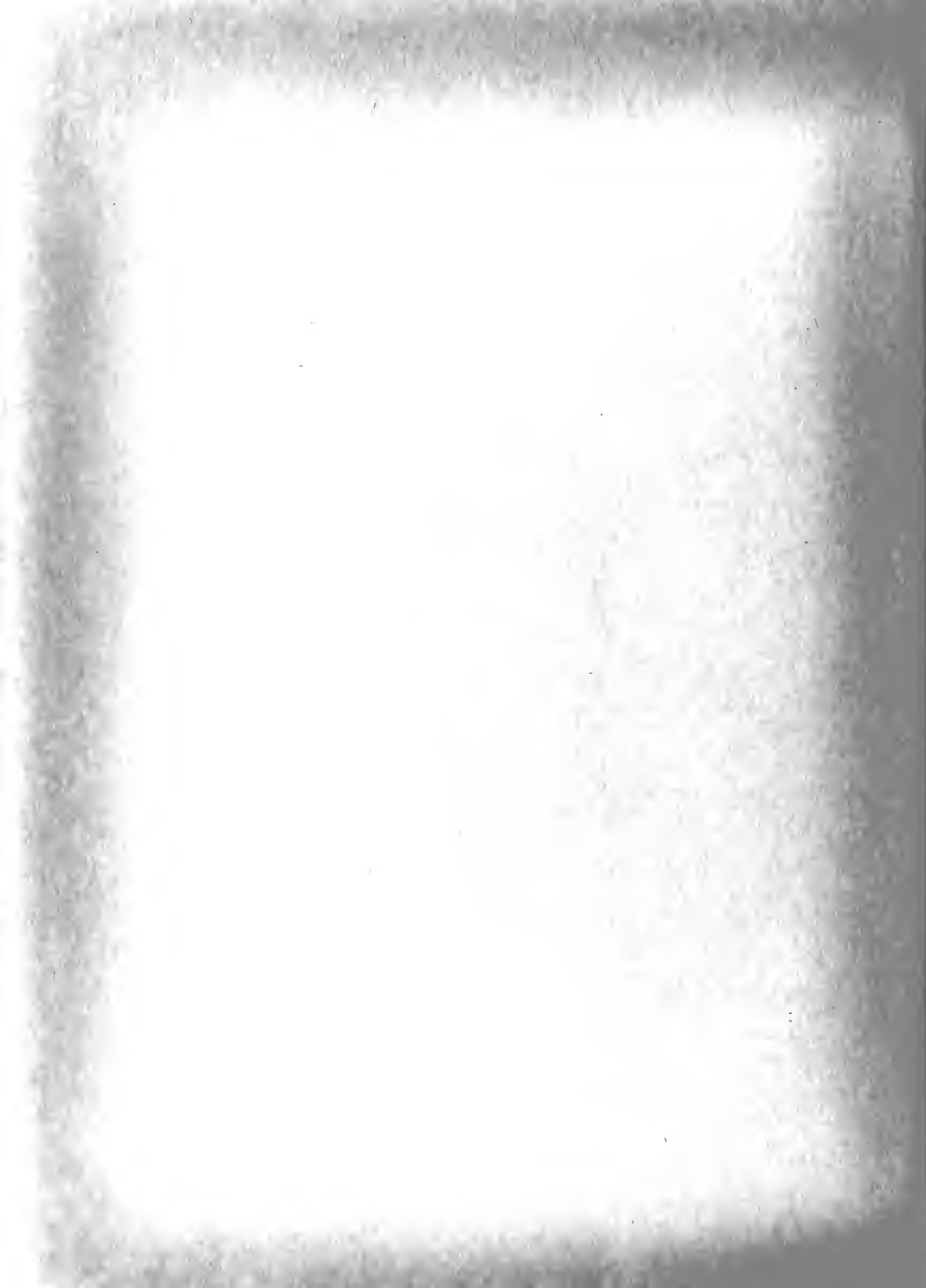
The transformers were of the auto type and were designed by General Electric personnel for this specific purpose. The function of the transformers is to lower the effective capacitance of the cable and thus the attenuation of the output pulse.

The transformers were of a 10 to 1 turns ratio, step down from the photomultiplier to the cable and step up from the cable to the amplifier. The specifications were that the transformers were to be used to connect 60 feet of RG 58/U cable of 28.5  $\mu\text{mfd}/\text{foot}$  or 1710  $\mu\text{mfd}$  total capacitance to the output capacitance of the photomultiplier. The frequencies to be passed ranged from 250 kc to 2 mc, thus the output impedance of the phototube covered from approximately 6400 ohms to 800 ohms.

The assembled connecting network had a 13  $\mu\text{mfd}$  shunt capacitance as seen from the high side and the output pulses reached the amplifier without excessive attenuation. However the pulse shapes as observed at the amplifier output indicated an undesirable amount of distortion which was attributable to the transformers. Also, in order to obtain the desired pulse amplitude the gain of the photomultiplier was increased by using a high voltage of -1826 volts. This is above the voltage at which photomultiplier tube noise becomes noticeable.

#### 4. AMPLIFIER

The remainder of the equipment consisted of commercially produced components and descriptions are available in the literature. It is felt, however, that the functioning of the amplifier and pulse height analyzer should be covered in order to describe how the spectrum is processed for analysis.



There are many commercial linear pulse amplifiers on the market. The type chosen for use in the spectrometer should have sufficient gain and a rise time short enough that the output will operate the various equipments used in analyzing, counting and registering these pulses. The amplifier should be noise free so as not to introduce counts of its own. The amplifier should be linear over the expected output range so as to avoid the necessity of calibration curves.

Several useable amplifiers were available in the laboratory. No one amplifier was outstanding in all respects when compared to the others. A final compromise was made in favor of the Atomic Instrument Company, Linear Amplifier, Model 204B, mainly because of its nearly linear characteristic over the desired output range, plus, of course, its acceptability with respect to noise.

A schematic diagram of the amplifier appears in Figure 14. The output pulse from the driving network is developed across a potentiometer and a fixed resistor. The potentiometer is a fine gain adjustment controlled by a dial on the front panel. There is also a coarse gain control determining the position at which the input to the grid of the first tube is taken off a voltage divider network. The coarse gain controls the amplitude of the input signal in steps of 6 db.

The signal, then, passes through differentiator networks determined by the "Rise Time" dial setting. The voltage pulse is differentiated so that it approximates the original pulse. The short time differentiation limits the use of the amplifier for slow rising pulses, but is good for gamma ray spectroscopy in that the rapid recovery time allows high





counting rates and is such that "gamma ray background will not"pile up" giving large pulse outputs. An internal switch is available for increasing the coupling capacitance in required cases.

From the coarse gain control the signal is supplied to the main amplifier. The main amplifier is composed of two separate three-stage amplifiers, each with its own feed back loop. The compensation is adjustable on both loops. The first stage feedback loop compensation is ganged so that it changes with the input differentiator network. The second stage feedback loop can be used to obtain satisfactory transient response.

The amplifier will take either positive or negative input pulses. Normally a positive pulse is desired. The "Input Polarity" switch, located on the front panel, can be used so that the input to the second stage will be taken from either the plate or cathode of the output tube of the first stage making the input to stage two always positive, thus, giving the desired positive output.

The maximum overall gain is not the product of the gain of each of the feedback loops but rather somewhat lower due to losses contributed by the differentiator and the output cathode follower. The output is available at either of two co-axial cable output connectors labelled "HIGH" and "LOW". The "LOW" output is intended to drive a co-axial cable with a maximum signal of about five volts, while the "HIGH" will deliver 100 volt signals without distortion.

The amplifier has a 300 volt supply which is well regulated to minimize gain variation and ripple.



## 5. PULSE HEIGHT ANALYZER

The pulse height analyzer used in the spectrometer is the Atomic Instrument Company, Model 510, consisting of an expander amplifier, two discriminators, and an anticoincidence circuit. The pulse height analyzer scans the energy spectrum, counting all pulses within a differential energy band, in such a way that the entire energy spectrum is scanned with no overlaps or skips.

The expander amplifier is comprised of a cathode coupled amplifier followed by a series-connected output stage. The initial tube is biased beyond cutoff by a voltage developed across a potentiometer controlled by the "BASE LINE" dial on the front panel. Any signal of amplitude larger than this base line bias has that portion of its signal which exceeds the base line amplified by a factor of 10. The amplified output of the amplifier expander is next fed to two discriminators.

The discriminators employed are of the conventional Schmitt trigger circuit type. The lower level, or base line, discriminator has its triggering level set so that a 5 volt output from the expander amplifier will cause it to trigger. This 5 volt triggering level referred back to the input requires a signal in excess of the base line bias by 0.5 volt for triggering the discriminator. A desirable condition would be one in which the discriminator triggered for any input exceeding the base line no matter how small the differential, however the input level of 0.5 volt was utilized in order that difficulties due to discriminator hysteresis might be avoided. When triggered, the lower level discriminator causes



a positive pulse of approximately 20 volts to appear at the plate of the output tube. The upper level, or channel width, discriminator has its triggering level set above that of the lower discriminator as determined by a potentiometer controlled by the front panel dial marked "CHANNEL WIDTH". The difference in triggering level can be varied from zero to 100 volts. Referred back to the input, this affords effective channel widths ranging from zero to 10 volts. Again, if the upper level discriminator is triggered an output pulse of approximately 20 volts appears at the plate of the output tube. The pulses from the two discriminators are sent to the inputs of a difference amplifier through a coupling network. For the proper functioning of the difference amplifier, output signals from the discriminators should be of the duration of one microsecond or greater. Difficulty arises here, in that the upper level discriminator may be measuring the top of a high-amplitude short-length pulse and its output may not be of the required length. In a conventional Schmitt circuit, the duration of the input and the output pulses are nearly equal. Therefore a pulse lengthening feature has been added to the circuitry of the channel width discriminator. The base line discriminator, with its low bias level and relative long time constant, acts as a univibrator with an output pulse of sufficient time duration. The amplitudes of the two discriminator outputs are adjusted to be identical.

In the anticoincidence circuit the outputs of the two discriminators are applied to the two grids of a cathode coupled difference amplifier. If the two grids have identical signals applied, no output is derived



from the difference amplifier. If only one grid receives a signal, and this can only be the first grid receiving a signal from the base line discriminator, the output taken at the plate of the second tube is a negative pulse. The output pulse can be adjusted as to amplitude by varying the plate load resistor.

As the gamma ray energy spectrum is scanned, there is an indication of the presence of gamma rays within the differential energy ranges. If the amplified gamma ray energies are below the base line level, neither discriminator is triggered and there is **no output**. If the lower level discriminator is triggered but not the upper, then the gamma ray energy is such that the amplified pulse is greater than the base line voltage, but less than the base line voltage plus the channel width voltage, or in other words, the gamma ray lies within the differential energy range just scanned. If the gamma ray energy is greater than the value of energy for either boundary of the differential energy range both discriminators trigger and the difference amplifier, amplifying the difference between the two identical discriminators outputs, has a zero value of difference to amplify and no output appears at the pulse height analyzer terminals.

## 6. ASSOCIATED EQUIPMENT

The signal has been traced from the sample through the pulse height analyzer. The signal out of the pulse height analyzer can be adjusted to any reasonable desired amplitude. There will be a number of output pulses at each gamma ray energy level proportional to the number of gamma rays given off by the sample at that corresponding level. By counting the





pulses the analyst can obtain a measure of the activity at that gamma ray energy. The remainder of the equipment is used to facilitate the counting of the output pulses and the presentation of the data in the desired form.

The linear count rate meter, Mark 15, Model 15, produced by the Radiation Counter Laboratories, Inc., Figure 14, is a precision counting rate meter designed for use with a single channel differential analyzer such as that previously described. The instrument indicates directly the average rate of occurrence of randomly distributed pulses of various wave forms and amplitudes on a front panel meter. It also has an output connection for use with a recorder. The full scale counting ranges can be adjusted to meet ordinary requirements. The maximum counting range is 50,000 counts per second. When samples give a low number of counts per second, say below 100 counts per second, the linear count rate meter is not satisfactory and a scaler may be utilized for more accuracy. With low counts the random nature of the counts requires that a long time constant be placed on the count rate meter, making it difficult to accurately read the equilibrium point of the meter. Provisions for this contingency were made in the spectrometer but were not used during the course of this project and are not covered in this report.

The Minneapolis-Honeywell Regulator Company, Type 153, Elektronik Recorder was used as the recording component with the spectrometer. The paper upon which the spectrum is recorded is driven past a pen by a roller and gear drive arrangement. The rollers can be stopped and any desired reference point set as the zero energy level. The gears, by a clutch



mechanism, can be caused to drive the paper and a potentiometer according to a prearranged ratio. The potentiometer is a 50 k ohm potentiometer which by means of a switch, can be substituted for the 50 k ohm potentiometer controlling the base line in the pulse height analyzer. As the base line moves, the channel width potentiometer keeps the desired separation between the triggering levels of the lower and upper level discriminators. In this way the energy spectrum is scanned. The distance along the time axis on the chart paper is proportional to gamma ray energy. The position of the pen carrier along a line parallel to the roller axis and contacting the paper at the roller surface is determined by the output of the linear count rate meter. Thus, a mark is made on the paper at a point corresponding to the gamma ray energy and the number of counts per unit time. By recording pertinent data, the analyst can compute the proportionality and thus analyze the spectrogram presented by the recorder. Spectrograms as presented by the recorder are shown in Figures 4a and 4b.

A Tektronix Cathode Ray Oscilloscope, Type 511 AD was utilized in monitoring the output of the amplifier. From the trace, as seen on the oscilloscope face, information can be obtained as to pulse shape, pulse amplitude and resolution. Figures 7a and 7b are reproductions of Polaroid pictures of oscillographs of  $\text{Co}^{60}$  and  $\text{Cs}^{137}$ . In the  $\text{Co}^{60}$  oscillograph one vertical division is equivalent to 10 volts or one Mev, one horizontal division equals one microsecond. The two gamma ray energy pulses at 1.17 Mev and 1.332 Mev and their summation pulse at 2.502 Mev are apparent, as are the less intense Compton pulses ranging from the summations peak



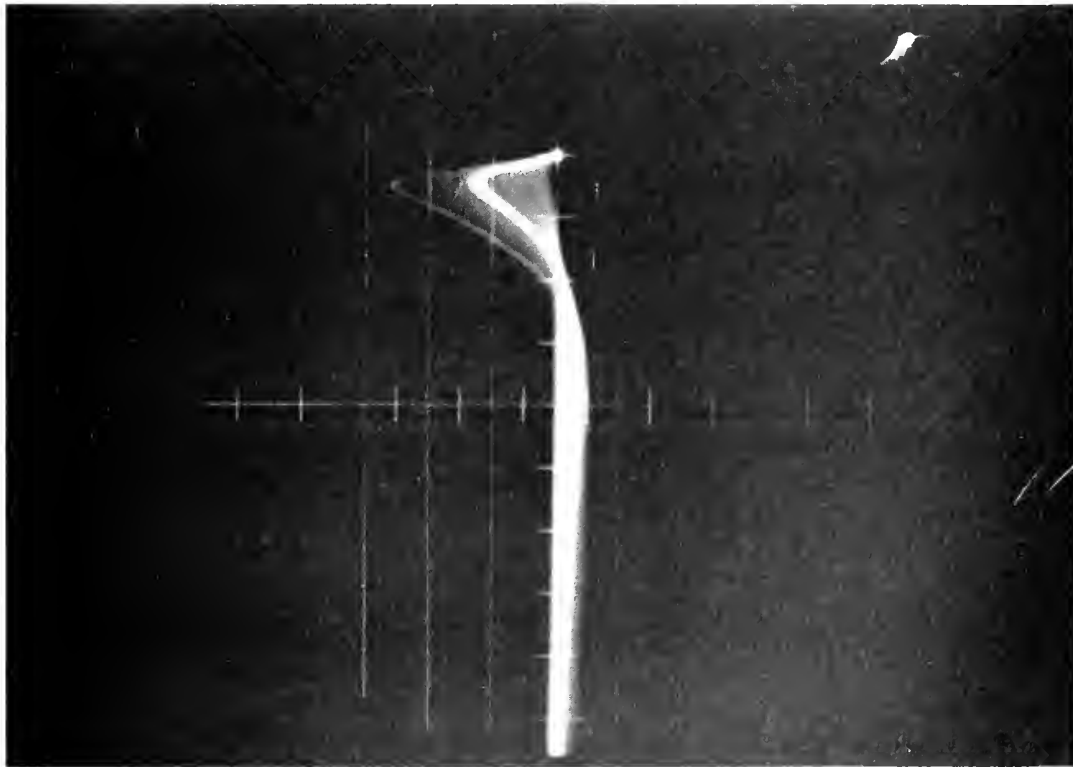


Figure 7a. Oscillograph of  $\text{Co}^{60}$  Spectrum

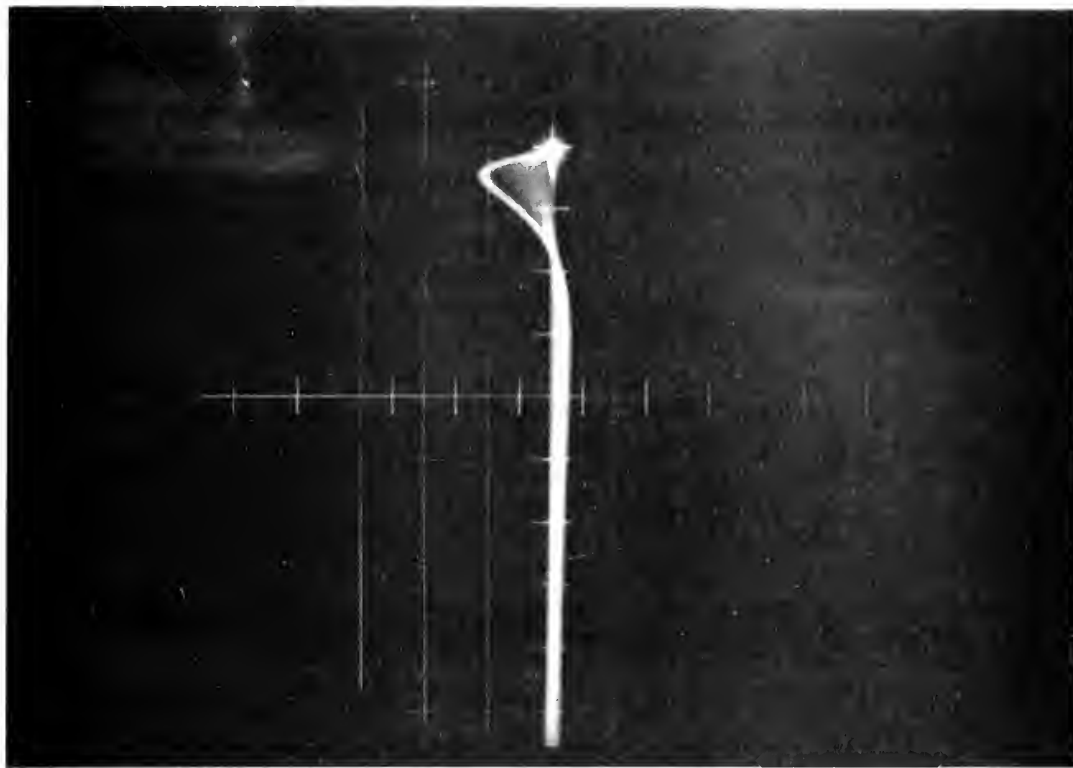


Figure 7b. Oscillograph of  $\text{Cs}^{137}$  Spectrum



down to zero energy. In the Cs<sup>137</sup> oscillograph one vertical division corresponds to five volts or 0.5 Mev and one horizontal division, again, equals one microsecond. The pulse from only one gamma ray is apparent at 0.66 Mev with the less intense Compton peaks ranging down to zero.

Figure 8 is a photograph of the spectrometer assembly including the amplifier, pulse height analyzer, linear count rate meter, oscilloscope and recorder located on the upper level.





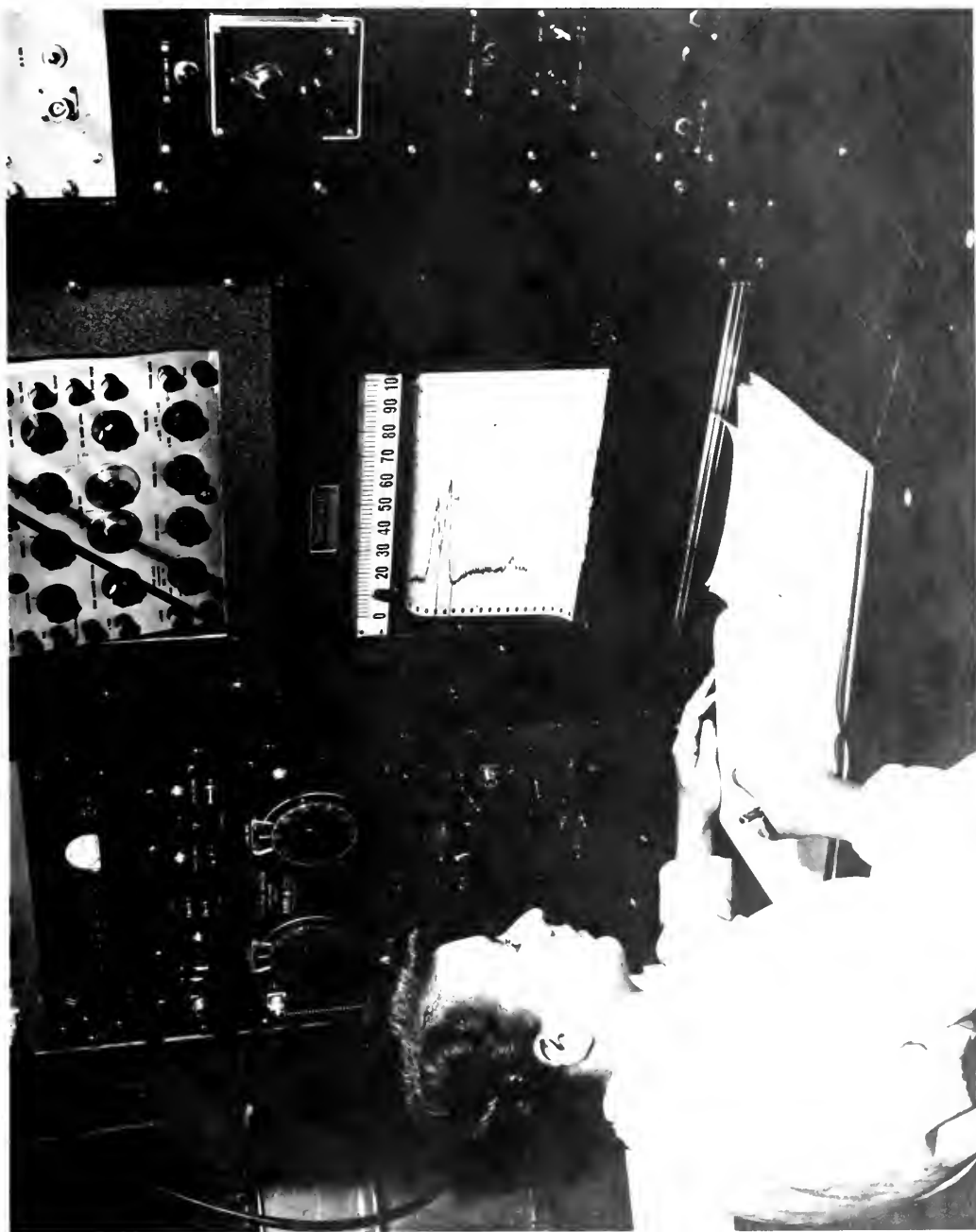


Figure 8. Main portion of spectrometer including amplifier, pulse height analyzer, linear count rate meter, recorder and oscilloscope.



CHAPTER V  
DRIFT IN THE GAMMA RAY  
SPECTROMETER

The drift which appeared in the gamma ray spectrometer consisted of an undesired displacement of the counting peaks in the energy spectrum. For accuracy and expediency in analyzing the scans of gamma ray spectra, it is desirable to have a spectrometer system in which a standard or several standard energy lines can be initially calibrated and set into the system and not change over the period of time during which a sample is being analyzed. If the standard energy lines remain stationary and if a convenient scale is chosen during calibration, the gamma ray energies of the sample can be read directly from the spectrogram obtained. With a constant reference point, valuable time is not lost in recalibration procedures between runs. With no recalibration necessary the operating conditions for the various electronic components remain unchanged and data is more consistent.

The drift problem encountered in the spectrometer described can best be illustrated by citing data obtained over a period of time (approximately 39 hours). A  $\text{Co}^{60}$  sample was placed in the crystal and left there throughout this phase. The high voltage was set during the initial calibration and undisturbed thereafter, as were all other dial settings on electronic components. Thus the only obvious variables were time and temperature. The  $\text{Co}^{60}$  gamma ray energy spectrum was scanned at random intervals throughout the period. The shift of the 1.172 Mev and 1.332 Mev gamma ray



peaks was taken as the measure of drift in the system. The two peaks followed the same drift pattern in general, however there are discrepancies in the drift of the two if one looks very carefully. Thus, there is evidence of drift taking place in the few seconds required to scan the portion of the spectrum between the 1.172 Mev and 1.332 Mev energy levels. The data is tabulated in Table 1 and appears in graphical form in Figure 9. During the period of observation recorded in Table 1 and Figure 9 the drift did not go to its extremes as observed by the writer. At one time, within a four hour period after calibration, the 1.172 Mev peak was observed to drift down to a position at 0.93 Mev. The drift error at times, then, may reach magnitudes of approximately 20%.

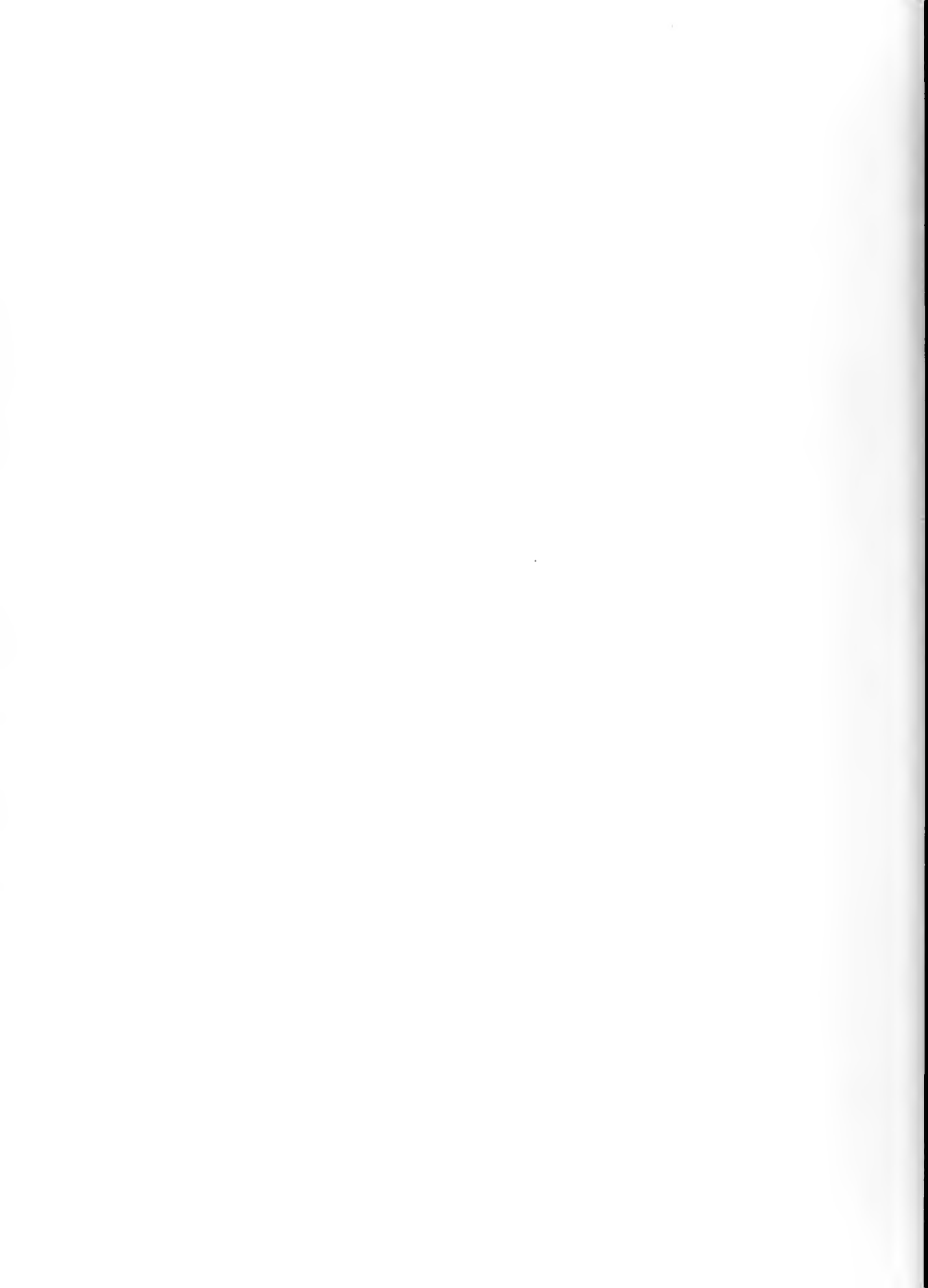
It is apparent that the drift of the spectrometer is neither consistent nor predictable. The erratic characteristic of the drift makes it even more undesirable. One can not be sure, even if the scan is made immediately after calibration, that a gamma ray energy peak will fall in its proper position on the spectrogram.

An analysis, by neutron activation methods, of a sample containing many trace elements would, normally, furnish a gamma ray energy spectrum with peaks fairly densely scattered throughout. As an example, studies of the trace element content of various biological tissues would entail analysis for some 50 elements [21] whose associated gamma ray energies lie in close proximity in many instances. This sort of analysis would be very difficult if the proportionality between the time axis and the gamma ray energies were not maintained. An effort to eliminate drift from the system led to modifications of the spectrometer as described in the following chapter.



Time in minutes since initial calibration	1.17 Mev gamma -ray occurred at ____ Mev	% drift from position at initial calibration	1.332 Mev gamma -ray occurred at ____ Mev	% drift from position at initial calibration
0	1.17	0.0	1.32	0.0
15	1.18	0.855	1.33	0.758
965	1.12	-4.270	1.28	-3.032
990	1.14	-2.565	1.29	-2.274
1020	1.13	-3.420	1.26	-4.550
1050	1.03	-11.980	1.16	-12.110
1080	1.06	-9.400	1.19	-9.850
1110	1.08	-7.680	1.22	-7.580
1140	1.12	-4.270	1.27	-3.790
1170	1.18	0.855	1.33	0.758
1200	1.18	0.855	1.33	0.758
1380	1.19	1.710	1.34	1.515
2405	1.12	-4.270	1.27	-3.790

Table 1. Tabulation of data for the determination of drift in the gamma-ray spectrometer.





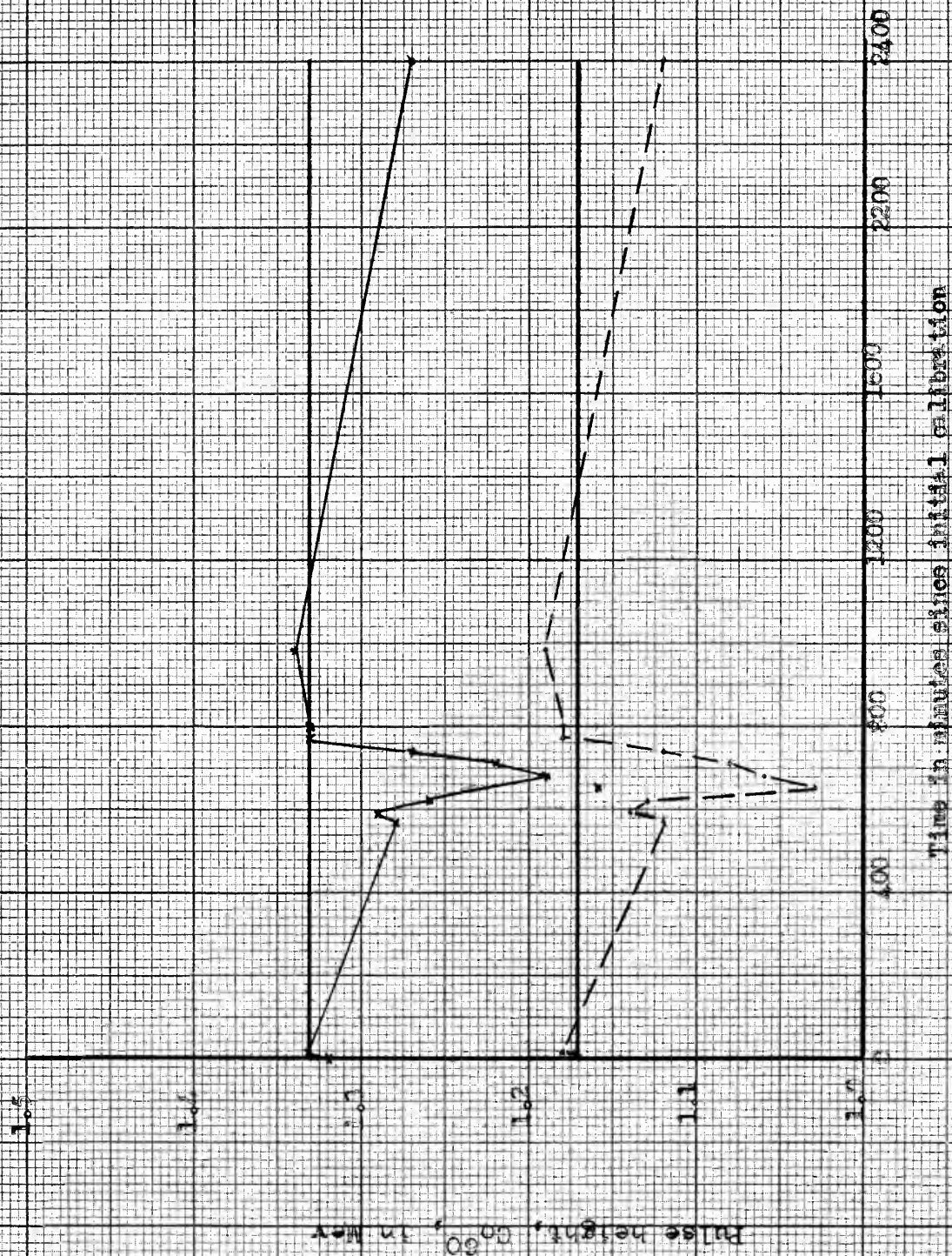


Figure 2. Drift characteristics of spectrometer before correction



## CHAPTER VI

### ELIMINATION OF DRIFT IN THE GAMMA RAY SPECTROMETER

In Chapter IV it was noted that all electronic units, such as the photomultiplier, power supply, amplifier, etc... were tested for any obvious detrimental effects which they might contribute to the system as a whole, before being adopted for use. These effects were mainly non-linearities and excessive noise. Where possible, noise was eliminated or reduced. For example, when hum, microphonics, extraneous transient pickup, or noise from defective components was the source of noise, it was possible to alleviate the situation. Noises such as resistor noise, grid current noise and shot-effect noise within the amplifier were found to be the final determining factors for signal-to-noise ratio during normal operation, and a combination of positive ion feedback and thermal noise within the phototube at higher voltage operation. The circuits for use within the spectrometer were chosen then on the basis of their near linear performance and minimum noise contribution. In light of the data presented in Chapter V it becomes essential to reevaluate the electronic units in terms of their drift stability.

Because a reliable pulse amplifier was essential to the testing procedure for other equipment, it was the first to be examined. Routine gain stability tests covering a period of 26 hours were performed. During the tests, 11 values of output, covering the expected range of output pulses (0 to 50 volts) from the amplifier were observed. The characteristics of the amplifier were such that less than 0.5% drift occurred during the



period. The deviation from linearity during the tests was on the order of 4%. Thus the pulse amplifier, while not the cause of the drift, seemed to be the main contributor to nonlinearity in the spectrometer. Possibly the linearity problem could be improved by a more suitable choice of operating points, however, this nonlinearity was not the main culprit at this stage, and it was decided to extend the investigation on drift.

The pulse height analyzer, linear count rate meter, and the recorder were tested as one unit. A precision pulse generator was used to feed a signal through the pulse amplifier into the remainder of the circuit. At first some rather surprising results were obtained. However, these discrepancies were traced to misalignment of the pulse height analyzer. Following the alignment procedure as set forth in the instruction manuals for the equipment, the units were realigned and recalibrated where necessary. The range of expected inputs to the pulse height analyzer (same as the pulse amplifier output range) was covered by using three pulse amplitudes, one at either extreme and one in the middle of the range. At various intervals during a 48 hour period the base line of the recorder was set at zero and the pulse amplitudes observed. A given input pulse as recorded on the chart varied less than 1% from the position originally calibrated. Actually 1% is an error which could easily be expected as inherent in the zero calibration of the recorder and the setting of the pulse amplitudes in the pulse generator. These components were not the source of drift and this test gave a further check on the reliability of the pulse amplifier.



Three units remained to be tested, the NaI(Tl) crystal, the multiplier phototube, and the power supply for the phototube. The crystal has its characteristic inaccuracies but these are mainly connected with a dropping away from linearity when detecting heavier particles and the deliquescent nature of the crystal. For detecting gamma rays the crystal is quite linear and the method of packing devised by Harshaw Company has kept the crystal free from any evident deterioration due to deliquescence. The deterioration could cause a change in the conversion efficiency, (gamma ray energy-to-light pulses), but this would be a very slow type of drift, always in a given direction, as opposed to the transient **unpredictable** drift which it is desired to correct.

The power supply, a Beva Laboratories, Model 302, 2.6 kilovolt power supply for the photomultiplier was tested by observing the voltage across a 1018 ohm precision resistor monitor provided in the voltage divider network. This voltage was used as one leg of a bridge, the other being the voltage across a 1.01802 volt Weston Standard Cell with a suitable voltage divider network. A galvanometer with a sensitivity of 0.077 microamperes per division was the null reading meter (no current flow between the two points, no voltage differential) in the third leg. The power supply was monitored for 18 hours and the maximum drift was 0.757%. This took place immediately after turning on the power supply. After an initial period of 20 minutes the maximum drift was 0.079%.

The effects of voltage variation on pulse height amplitude were next examined. A change of high voltage of 1.08% was observed to cause a drift of 6.5%. If the power supply is given adequate time to warm up (it normally is left on continuously, without high voltage being applied



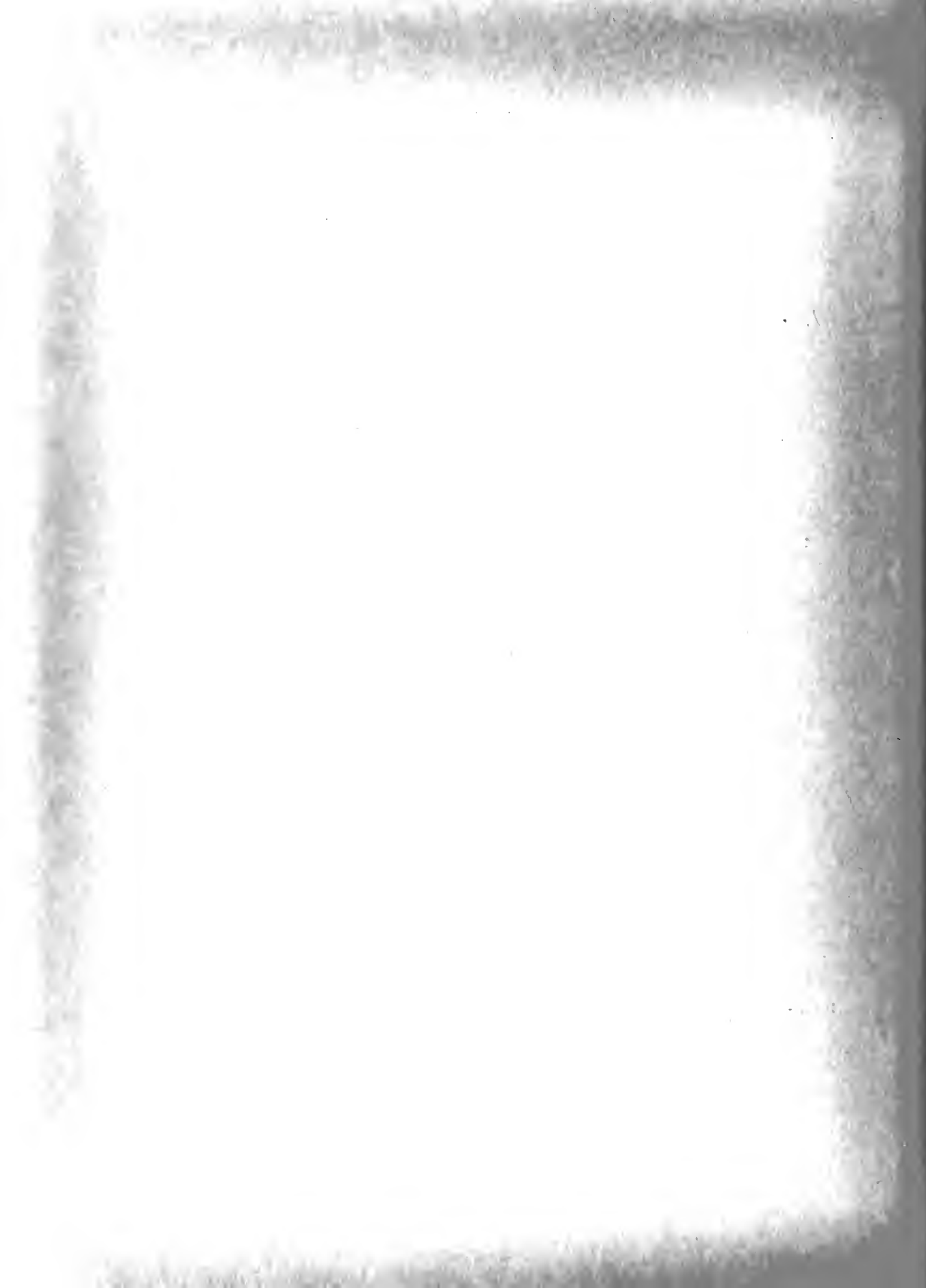


to the photocell) the maximum shift in pulse amplitude would be of the order of 0.475%. Therefore we conclude that power supply stability characteristics are satisfactory.

The multiplier phototube was the last of the system to be tested, and it would seem, by a process of elimination, the offending unit had been isolated. Tests were run with the tube picking up the scintillations caused by the  $\text{Co}^{60}$  gamma rays. The  $\text{Co}^{60}$  sample was placed in the crystal well and the tube was coupled in the normal manner. The power supply was connected in the usual fashion and the peaks were observed to drift unpredictably, the maximum drift being about 20%.

The phototube was being operated in this case at -1826 volts, which is at the upper limit specified by the manufacturer. If this voltage is applied directly to the bleeder network the voltage between dynode stages is approximately 131 volts and between photocathode and dynode #10 is 522 volts. This interdynode potential should, according to the specifications, give an overall current amplification of about  $1.6 \times 10^6$  which is a relatively high gain.

A major disadvantage of photomultiplier tubes, in general, lies in the fact that the secondary emission ratio is not an absolute constant. When the accelerating voltage of primary electrons is increased, the secondary emission ratio increases to a certain point and then decreases again. This phenomenon occurs because at low primary energies the energy available for excitation is low and the yield of secondary electrons is thus low; at very high primary energies the primary electron does most of its ionizing after it has been slowed down, that is, after it has



penetrated deeper within the secondary emitter material, and the freed electrons lose their energy before escaping. After reaching this point, any further increase in voltage will cause a decrease in the secondary emission ratio.

Several other characteristics of photomultiplier tubes are noteworthy at this point. These characteristics include:

- (a) Thermionic emission,
- (b) Positive ion bombardment,
- (c) Light feedback,
- (d) Charging of the glass envelope,
- (e) Ohmic leakage within the tube and
- (f) Voltage divider resistance variations.

These will be discussed in some detail.

Thermionic emission of electrons from the photocathode and dynodes may contribute to the phototube output. Operating the tube at temperatures of around  $30^{\circ}$  Centigrade, thermionic emission could be expected since the work function, especially for the photocathode material, is low. The output due to this thermionic emission,  $i_{th}$ , will be proportional to gain,  $G$

$$i_{th} = K_1 G \quad (14)$$

since these electrons are multiplied in the same manner as those due to photoemission.  $K_1$  is a constant of proportionality. Gain, in turn, is given by the relation

$$G = R^n \quad (15) \quad [1]$$

where  $n$  is the number of stages and  $R$  the secondary emission ratio. If



we assume that  $R$  is constant at a given interdynode voltage,  $V$ , and is proportional to  $V$ , that is

$$R = K_2 V$$

where  $K_2$  is another constant of proportionality. Then

$$G = R^n = K_2^n V^n$$

for all stages having the same voltage difference, as is the case in the spectrometer. This can be written

$$A = K_2^n \left( \frac{V_o}{n-1} \right)^n$$

where  $V_o$  is the overall voltage. The thermionic contribution becomes

$$i_{th} = K_1 G = K_1 K_2^n \left( \frac{V_o}{n-1} \right)^n \quad (16)$$

Thus thermionic emission output increases much faster than voltage.

In the literature [6] it is mentioned that with higher voltages regenerative effects may occur. In a cesium antimony, Cs-Sb, photomultiplier tube regeneration may occur at interstage voltages over 110 volts, and may cause a tube to become completely unusable. [1]

Positive ion bombardment of the dynode and photocathode surfaces also increases with an increase of interdynode voltage. The energy of the electrons passing through the phototube increase with the voltage. These electrons will at some potential gain enough energy to ionize the residual gases within the tube. The ions, usually positive, will be attracted to the more negative parts of the tube such as the dynodes and photocathodes. When they strike these surfaces they cause secondary emissions which add to the signal pulse and background noise. The ionizing effect should be greatest when the largest number of electrons are flowing through the tube, that is during a pulse. At the same time the distribution



of residual gases and the position in the tube where ionization takes place would be variable. If a positive ion were formed near a dynode surface it would strike that surface and cause secondary emission during the pulse, thus, contributing to the pulse amplitude. If the ion were formed at some distance from the dynode it would strike later contributing an after pulse. Furthermore, if positive ion bombardment takes place at dynode #1 the contribution would be greater than if it took place at dynode #10, since the former would experience 9 stages of multiplication while the latter would experience none.

Light feedback occurs when electrons strike various portions of the multiplier structure causing them to emit light. This again would be more likely with higher electron energies and therefore would occur at higher voltages. The effect is of consequence only if the light is seen by the photocathode, thus it can be minimized by shielding the cathode or, alternatively, depressing the fluorescent properties of the various structures. Most tubes are manufactured in such a way that light feedback is not a worrisome factor.

It has been reported by various sources that if metallic bodies at anode potential are in close contact with the tube envelope tube noise increases, large spurious pulses are detected and that, at times, the output of the tube may become unstable [4]. The effect does not, to the knowledge of this writer, have its explanation in any set theory. However, the common belief is that it arises from discharges between the inner surface of the tube envelope, which tends to be at cathode potential, and the metal at anode potential. The discharge results in a light pulse which feeds back to the photocathode. During high voltage





operation the photomultiplier is enclosed in a light tight container, since normal light intensities would result in destruction of the tube. Therefore, the discharge arc has not been observed by the author. It is conceivable that the arc might be a much more intense flash than the normal scintillations, and of longer duration. A flash of this type can cause a fatigue effect such as that mentioned by R. Davis, P. Bell, and W. Bernstein [2] in which a photomultiplier exposed to an intense flash will drift away from its normal amplification characteristics. The fatigue effect was demonstrated by the author by placing an intense  $\text{Cs}^{137}$  source close to the well and observing the drift of the 0.66 Mev gamma ray peak. Fatigue effect as reported in the literature can either lower or raise the gain, though in most cases reported lower gain results. This would seem to tie in with the spectrometer drift which for the most part tends to be downward. This effect is temporary and the tube returns to normal after the intense source has been removed.

Because of the relatively high voltage between elements there will be some leakage across the supporting insulators of the multiplier structure. This effect is called ohmic leakage and again will increase with increased voltage. During the process of coating the dynode surfaces some of the cesium vapor condenses on the insulator supports [14] forming a conduction path. These cesium deposits, especially thin film types, are very unstable, and the resulting leakage fluctuates in value. That is, as heavy currents are drawn, cesium deposits tend to migrate [4] giving variable conduction paths. As a matter of fact, the cesium deposited on the dynodes seems to exhibit this same characteristic at



high current values and affects the secondary emission ratio, thus affecting the electron multiplication.

The last effect mentioned was voltage divider resistance variations. The voltage divider network is in close proximity to the phototube where the temperatures may change. If the resistance of each resistor in the network changes in the same ratio with temperature changes, the interstage potentials do not change. Low-valued wire wound resistances are satisfactory in this respect. However, when large-valued composition resistors are used, as in the spectrometer, this is not the usual situation [23] and any variations in the interstage voltages will affect the overall gain and thus the pulse height of the phototube output.

The above enumerated effects are all, in one way or another, detrimental to the operation of the photomultiplier tube. They may all contribute in different degrees to the problem of drift, the exact percentage contribution would be extremely difficult to determine under normal laboratory conditions. It seemed to the author that the listed effects were all aggravated by high voltage operation and that certain of these effects contribute to variable gain within the tube. Thermionic emission had an effect dependent on the overall voltage, but it would seem this would appear as noise scattered throughout the spectrum. Positive ion bombardment, being more predominant with the high voltage and heavy currents, appears to be the major factor in drift of a variable nature. Light feedback is a function of high voltage, but tube construction has probably depressed this to a nearly negligible quantity. Discharges between metallic bodies and tube envelopes might well cause



fatigue effect drifts since the photocathode is at -1826 volts and the crystal holder and enclosing case for the crystal-multiplier phototube are at ground potential (anode potential). Cesium deposit migrations with larger currents cause drift of the gain characteristics, and resistance variations may also shift gain. The last two are probably minor factors contributing to spectrometer drift.

The photocathode output was observed with various voltages applied to the phototube. These voltages ranged from 500 to 1800 volts. The period of observation was five hours. A convenient reference point in the  $\text{Co}^{60}$  spectrum was initially noted and the drift from this point was converted to a percentage drift. It was found that below 1100 volts the output drifted less than 2.5%, while above 1400 volts the drift became very erratic and reached a maximum drift of 20% at 1800 volts, see Figure 13. The next step was to devise a way to operate at lower voltages.

High voltage, high gain operation of the phototube was essential to obtain a usable signal at the amplifier input, after attenuation in the long coaxial cable. The auto transformers were used to minimize the effect of the distributed capacitance to ground. This was effective over a small range of frequencies. However, to pass the output pulse a wide band would be needed. In addition the transformers were distorting the signal pulse. Therefore it was decided to attempt a solution by amplifying the signal as near as possible to the photo-multiplier output, enabling lower gain and lower voltage operation of the tube. It was also decided to change the polarity of the high



voltage applied to the phototube, placing the cathode at ground potential with the surrounding metallic bodies and the anode at positive high voltage. This last step should eliminate the metal to envelope discharge which has been reported to cause output instability.

Changing the polarity of the high voltage and rewiring the phototube for application of high voltage to the anode were relatively simple procedures. The final configuration is as illustrated in Figure 14 by solid lines. The dashed lines show the initial configuration for negative high voltage to the photocathode.

Rather than placing the entire amplifier near the phototube, it was decided to divide the overall amplification of the photomultiplier signal between a "main amplifier" and a "preamplifier". The Atomic Linear Amplifier, Model 204-B originally used, remained with the main body of the spectrometer as the main amplifier. A preamplifier was designed for placement near the photocathode. The schematic of this preamplifier appears in Figure 12.

The need for stability led to the choice of a feedback loop similar to the one cited by Elmore [5]. Referring to Figure 12, a negative signal at  $V_1$  causes the plate of  $V_1$  to rise in potential. This rise introduces a positive input at the grid of  $V_2$  which is accompanied by a drop at the plate. The negative signal at the plate of  $V_2$  is directly coupled to the grid of  $V_3$ . Elmore uses this stage as a cathode follower, the output signal being negative. In the present case it was desired to invert the signal so that the preamplifier output would be a positive pulse. To accomplish this a resistance was placed in series









with the plate of  $V_3$  and the output signal taken from the plate. The negative signal at the grid of  $V_3$  tends to decrease the plate current through  $V_3$ , thus lowering the voltage of the cathode of  $V_3$ . This voltage drop of the cathode is feedback through the direct coupled feedback network to the cathode of  $V_1$ . The feedback is degenerative since a negative signal at the grid of  $V_1$  is offset by the drop of the cathode due to the feedback, the feedback tending to counteract the effect of the original signal. There is also cathode degeneration for  $V_1$  due to the flow of the conduction currents of  $V_1$  and  $V_3$  through the unbypassed 47 ohm resistor at the cathode of  $V_1$ .

Exact circuit analysis for the transient behavior of the loop is so involved that design of such elements have normally been by trial and error procedures. Elmore states that the gain of such a loop is given within 5% by the ratio

$$G = \frac{R_1 + R_2}{R_2}$$

$R_2$  is chosen for proper cathode biasing of  $V_1$  as well as to determine the gain. In the case of the spectrometer the gain becomes

$$A = \frac{65 \times 10^3 + 47}{47} = \frac{6547}{47} = 139$$

Experimental verification of this gave a gain of 131. The discrepancy most likely is due to the departure of the resistances from their normal values, and the variation of tube characteristics. The capacitance in the feedback loop facilitates the feedback of high frequency components producing good transient response. The output of  $V_3$  is fed to a slightly different type of cathode follower arrangement.



$V_4$  is a cathode follower having as part of its cathode load an active element  $V_5$ . A positive signal at the grid of  $V_4$  would cause an incremental current to flow in the direction of the cathode through the tube to the plate, an increase in plate current. With an increase in plate current the cathode of  $V_4$  would tend to rise, following the grid. The plate of  $V_4$  would drop in potential as would the screen grid, introducing a negative signal on the grid of  $V_5$ . This signal would tend to cause an incremental current to flow from the plate of  $V_5$  through the tube toward the cathode, a decrease in plate current. The effect on the output circuit is the sum of the two incremental current changes, see dashed arrows, Figure 12. That is, the effects of the two tubes add, a greater current change is produced, and the output impedance is effectively lower than for a normal cathode follower stage. This is a very effective output stage for driving the long coaxial cable. The gain of the cathode follower is something less than one, however, this is not of consequence since the preamplifier gain has been made large enough that the desired signal has been obtained.

Great care was taken in wiring the preamplifier in order that stray wiring capacitances be held to a minimum. The 6AK5s were chosen because of their low input capacitance, of the order of  $7 \mu\text{fd}$ . A pentode rather than a triode was desired for the input tube. A triode with its coupling between plate and grid results in a lower input impedance due to Miller effect. The shielding in a pentode reduces this coupling to a negligible amount. The cable used to bring the signal from the photomultiplier output to the preamplifier input was type RG 114/U, which was the lowest



capacitance cable the writer could find. The capacitance of the RG 114/U is  $6.5 \mu\text{fd}/\text{ft}$ . One foot of the cable was used. With the design mentioned and careful consideration to construction procedures a high input-impedance, low output impedance, stable preamplifier was obtained.

The overall gain of the preamplifier was approximately 110, and the linearity and drift characteristics were satisfactory. With the signal preamplified before driving the cable, the photomultiplier gain could be decreased. The new operating voltage for proper calibration of the pulse heights of  $\text{Co}^{60}$  was found to be 892v, or approximately 64 volts between dynode stages, and 255 volts between the photocathode and first dynode stage.

Drift characteristics of the gamma ray spectrometer were now observed for a period of nine hours. The results of these runs are given in Table 2 and Figure 10. The maximum drift occurring was 1.122%.

The modification was considered very successful except for an increase of noise background. It was observed that the noise level rose and fell when the beatatron was operating at the other end of the building. The preamplifier seemed to be very susceptible to external transient pickup. Perforated metallic sheets were fastened to the bottom, top and sides of the chassis. With this shielding the noise level dropped to a level lower than that which had been encountered in the unmodified spectrometer. This, too, was attributed to the low voltage operation.

The duplication of results was the next item to be investigated. It was found that by placing index marks at the various settings corresponding to the original calibrations and returning to these marks after inoperative





Time in minutes since initial calibration	1.17 Mev gamma ray occurred at — Mev	% drift from position at initial calibration	1.332 Mev gamma ray occurred at — Mev	% drift from position at initial calibration
0	1.17	0.0	1.34	0.0
15	1.165	-0.427	1.33	-0.747
60	1.175	0.427	1.34	0.0
120	1.17	0.0	1.33	-0.747
950	1.16	-0.855	1.325	-1.122
990	1.165	-0.427	1.33	-0.747
1020	1.17	0.0	1.34	0.0
1080	1.17	0.0	1.33	-0.747
1110	1.17	0.0	1.33	-0.747
2140	1.175	0.427	1.34	0.0
2290	1.17	0.0	1.33	-0.747
2320	1.18	0.855	1.34	0.0
2350	1.17	0.0	1.33	-0.747

Table 2 . Tabulation of data for the determination of drift after modification of the gamma ray spectrometer



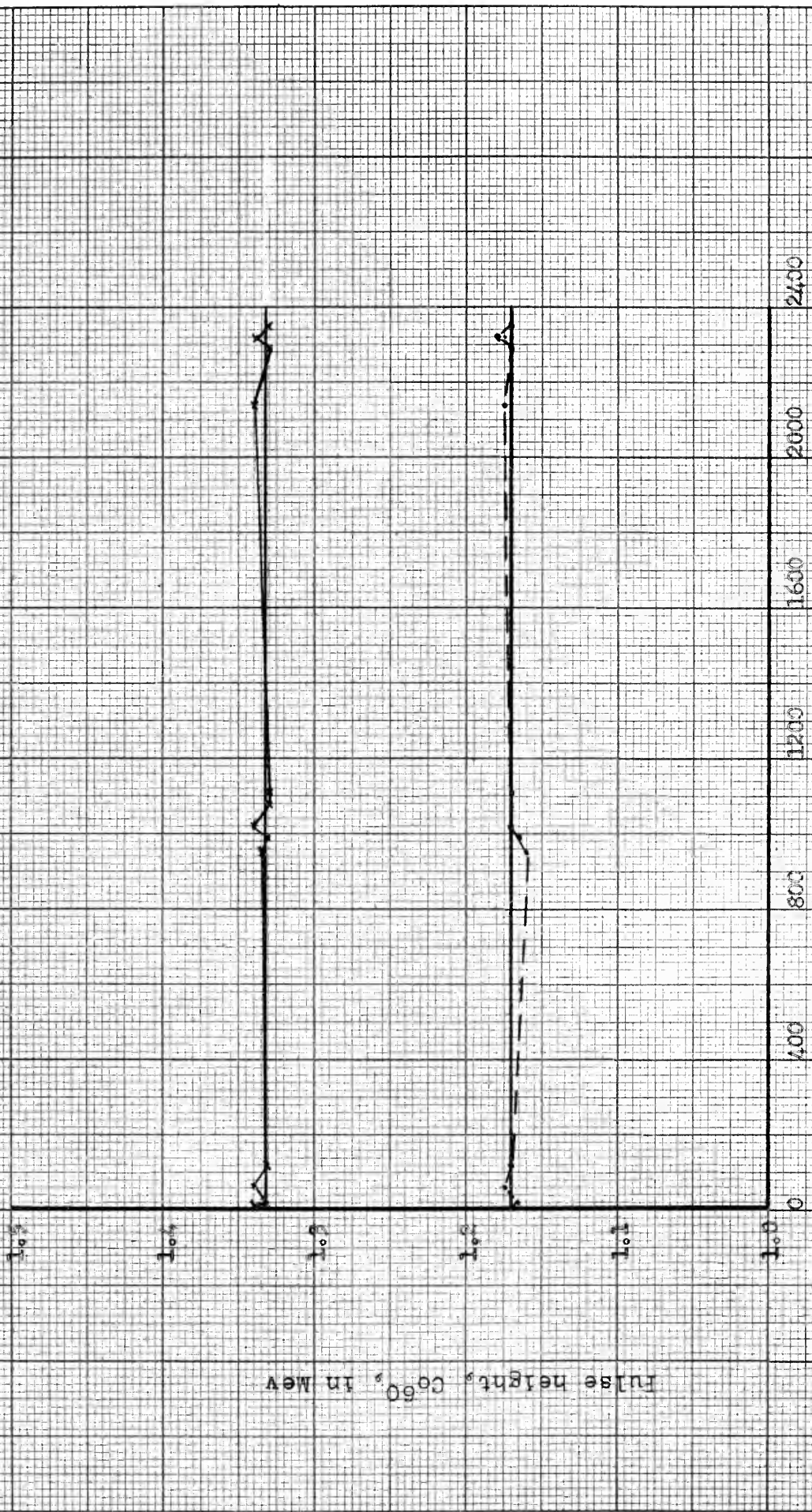


Figure 10. Drift characteristics of spectrometer after modification



periods results could be reproduced within 1.5% and further that the process worked in both directions. That is the setting of, say, the high voltage applied to the multiplier phototube at 892 volts would give an indication of a gamma ray energy for  $\text{Co}^{60}$  of 1.17 Mev on the chart, or the adjustment of the peak on the chart would end with a voltage in the range of 890 to 895 volts being applied to the phototube.

A block diagram of the modified spectrometer appears in Figure 11.



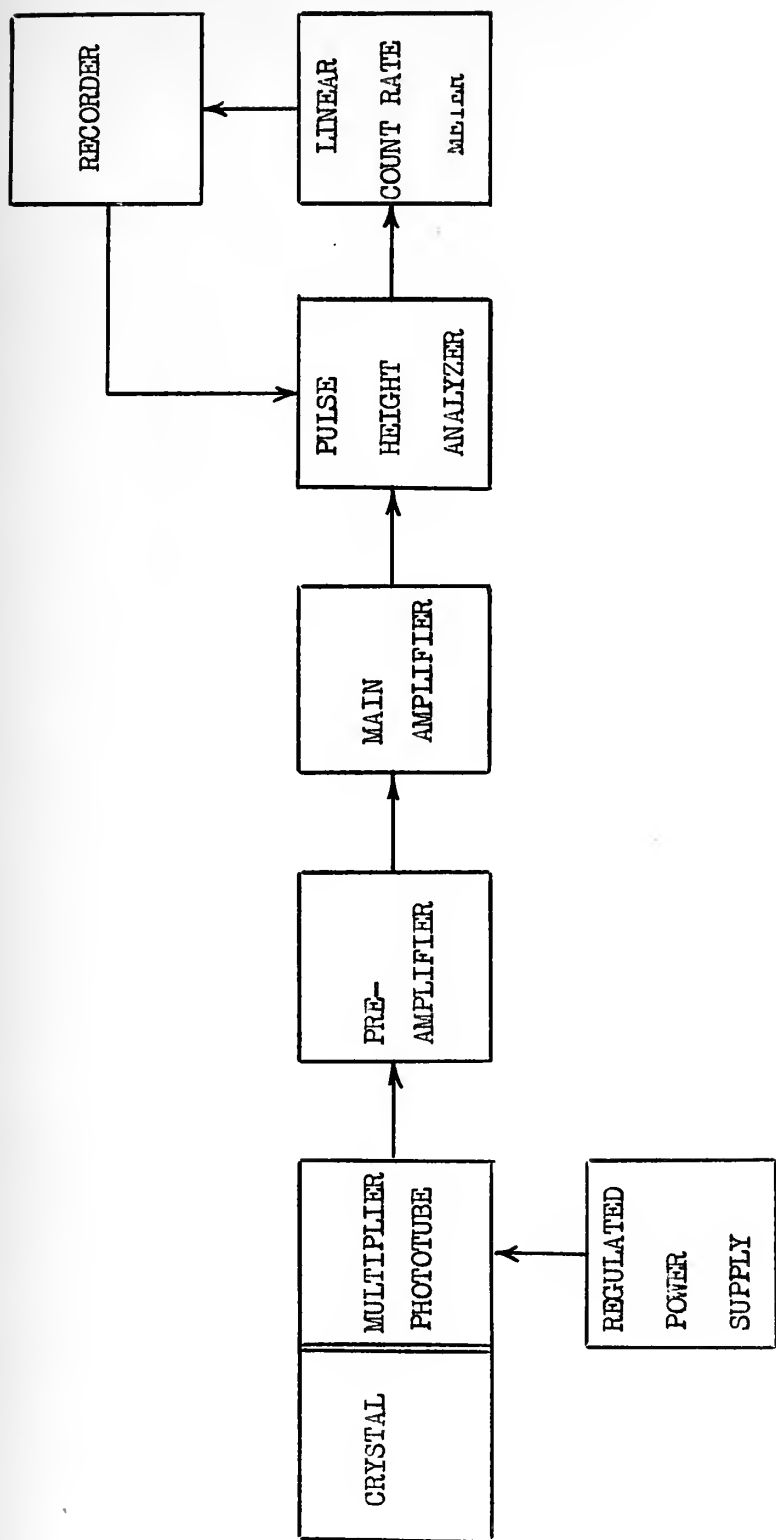


Figure 11. Block diagram of modified gamma ray spectrometer





## CHAPTER VII

### CONCLUSION

In light of the success of the drift elimination program as set forth in Chapter VI the spectrometer obtains three very desirable characteristics:

- (a) spectrograms run within the same 24 hour period will have a common reference point, as calibrated, within close tolerances,
- (b) time lost in recalibration is much reduced, and
- (c) conditions are reproducible.

Prior to leaving the General Engineering Laboratory the writer had a chance to work with a prototype linear pulse amplifier developed at the West Lynn plant of General Electric. The circuit was tested and found to be as stable as the amplifier in use in the spectrometer. In addition the West Lynn amplifier was much more linear in the range of energies normally covered in activation analysis. The noise introduced by the amplifier was about half that of the best of the other amplifiers tested and the resolution, as would be expected, was improved. It is believed a thorough study of this amplifier with the prospect of incorporating it into the spectrometer might be very beneficial.

The runs made on biological specimens indicated the potentialities of the system in this field, however they were not conclusive as to concrete analytical results. A detailed study of the optimum irradiation and detection procedures, keeping in mind the trace and bulk elements which most probably would be encountered, should enhance the method.



## BIBLIOGRAPHY

1. Armed Forces Special Weapons Project      NUCLEONICS FUNDAMENTALS, Headquarters Field Command, Armed Forces Special Weapons Project, Sandia Base, Albuquerque, New Mexico
2. Bell, P., Davis, R. and Bernstein, W.      PULSE HEIGHT VARIATION IN SCINTILLATION COUNTERS, Review of Scientific Instruments, Vol. 26, No. 7, 726, 1955.
3. Boyd, G.      METHOD OF ACTIVATION ANALYSIS, Analytical Chemistry 21, No. 3, 335-347, 1949
4. DuMont Laboratories      DUMONT MULTIPLIER PHOTO TUBES, Allen B. DuMont Laboratories, Inc., Clifton, New Jersey, 1955
5. Elmore, W.      ELECTRONICS FOR THE NUCLEAR PHYSICIST II (Second of a series of three articles) Nucleonics 2, No. 3, 16-36, 1948
6. Engstrom, R., Stoudenheimer, R., and Glover, A.      PRODUCTION TESTING OF MULTIPLIER PHOTOTUBES, Nucleonics 10, No. 4, 58-62, 1952
7. Eshbach, O.      HANDBOOK OF ENGINEERING FUNDAMENTALS, Wiley, 1952
8. Hevesy, A. and Levi, H.      Kgl. Danske Videnskab, Selskab Math-fys. Medd., 14, No. 5, 1936 (Royal Danish Society of Mathematics and Physics)
9. Hughes, D. and Harvey, J.      NEUTRON CROSS SECTIONS, United States Atomic Energy Commission, McGraw-Hill Book Company, Inc., 1955
10. Joliot, F. and Curie, I.      ARTIFICIAL PRODUCTION OF A NEW KIND OF RADIO-ELEMENT, Nature 133, 201-2, 1934
11. Leavitt, W. and Senftle, F.      ACTIVITIES PRODUCED BY THERMAL NEUTRONS, Nucleonics 6, No. 5, 54-63, 1950
12. Leddicotte, G. and Reynolds, S.      ACTIVATION ANALYSIS WITH THE OAK RIDGE REACTOR, Nucleonics 8, No. 3, 62-65, 78, 1950
13. Leddicotte, G. and Reynolds, S.      NEUTRON ACTIVATION ANALYSIS A USEFUL ANALYTICAL METHOD FOR DETERMINATION OF TRACE ELEMENTS, U. S. Atomic Energy Commission, AEC - 3489, 1953



14. Linden, B., Palmer, R. and Deichert, R. MULTIPLIER PHOTOTUBES, The Oscillographer, Vol. 14, No. 4, 3-15, 1954
15. Meinke, W. and Anderson, R. ACTIVATION ANALYSIS USING LOW LEVEL NEUTRON SOURCES, Analytical Chemistry 25, No. 5, 778-783, 1953
16. Muehlhause, C. and Thomas, G. USE OF THE PILE FOR CHEMICAL ANALYSIS, Nucleonics 1, No. 1, 9-17, 59, 1950
17. Olsen, K., Heggen, G., Edwards, C., and Gorham, L. TRACE ELEMENT CONTENT OF CANCEROUS AND NONCANCEROUS HUMAN LIVER TISSUE, Science 119, No. 3100, 772-773, 1954
18. Reynolds, A. PROPERTIES OF SCINTILLATION MATERIALS, Nucleonics 6, No. 5, 70-72, 1950
19. Siegbahn, K. BETA- AND GAMMA-RAY SPECTROSCOPY, Interscience Publishers, Inc., 1955
20. Taylor, T. and Havens, W., Jr. NEUTRON SPECTROSCOPY FOR CHEMICAL ANALYSIS III, (third of a series of three articles), Nucleonics 6, No. 4, 54-66, 1950
21. Tobias, C. and Dunn, R. ANALYSIS OF MICROCOMPOSITION OF BIOLOGICAL TISSUE BY MEANS OF INDUCED RADIOACTIVITY, Science 109, No. 2823, 109-113, 1949
22. Webb, L. THE EFFECT OF TEMPERATURE UPON THE RESPONSE OF A GAMMA-RAY SCINTILLATION SPECTROMETER, USNRDL - TR - 48, NS 081 001, 1955
23. Wilson, R. CONSTANCY OF PHOTOMULTIPLIER GAIN, Journal of Scientific Instruments, Vol. 30, No. 12, 472-474, 1953



# APPENDIX I

## TABLE OF SENSITIVITY COMPARISONS

The following is a table comparing the sensitivities obtained using the methods of activation analysis with five other typical methods. The data included in the table was compiled and presented by W. W. Meinke in the article, "Trace Element Sensitivity: Comparison of Activation Analysis with Other Methods", Science 121, 177-184 (1955).

Table 3. Sensitivity comparisons ( g/ml).

Z	Element	Methods					
		Oak Ridge LITR reactor	Copper spark	Graphite direct- current arc	Flame spectro- photometer	Sensitive color reaction	Ampero- metric titration
1	H						
2	He						
3	Li		0.002		0.02		
4	Be		.002		250.	0.04	
5	B		.1		10.		
6	C						
7	N						
8	O						
9	F		.1				0.25
10	Ne						
11	Na	0.00035	.1	20.	0.002		
12	Mg	.03	.01	0.1	1.	.06	
13	Al	.00005	.1	.2	20.	.002	300.
14	Si	.05	.1	2.		.1	
15	P	.001	20.	50.		.01	15.
16	S	.2					5.
17	Cl	.0015				.04	10.
18	A						
19	K	.004	0.1		0.01		100.
20	Ca	.19	.1		.03		100.
21	Sc	.0001	.005				
22	Ti		.1		2.	.03	10.
23	V	.00005	.05		2.	.2	3.
24	Cr	.01	.05	2.	1.	.02	1.
25	Mu	.00003	.02	0.2	0.1	.001	0.0003
26	Fe	.45	.5	.2	2.	.05	2.
27	Co	.001	.5		10.	.025	100.
28	Ni	.0015	.1	4.	10.	.04	0.5





Methods							
Z	Element	Oak Ridge LITR reactor	Copper spark	Graphite direct- current arc	Flame spectro- photometer	Sensitive color reaction	Ampero- metric titration
29	Cu	.00035		0.2	0.1	.03	10.
30	Zn	.002	2.	20.	2000.	.016	10.
31	Ga	.00035	1.		1.		
32	Ge	.002				.08	
33	As	.0001	5.	10.		.1	0.4
34	Se	.0025					
35	Br	.00015					200.
36	Kr						
37	Rb	.0015	0.2		0.1		
38	Sr	.03	.5		.1		
39	Y	.0005	.01		50.		
40	Zr	.015	.1			.13	
41	Nb	.5	.2		20.	50.	
42	Mo	.005	.05		30.	0.1	5.
43	Tc						
44	Ru	.005			10.	.2	
45	Rh				1.	.2	
46	Pd	.00025	.5		1.	.1	
47	Ag	.0055		0.1	0.5	.1	1.
48	Cd	.0025	2.	4.	20.	.01	5.
49	In	.000005	1.		1.	.2	100.
50	Sn	.01		0.2	10.		2.
51	Sb	.0002	5.	4.		.03	10.
52	Te	.005	0.5		100.	.5	
53	I	.0001					1.
54	Xe						
55	Cs	.0015	.5		1.		
56	Ba	.0025	.1		3.		25.
57	La	.0001	.05		5.		
58	Ce	.005	.5		20.	.25	500.
59	Pr	.0001	.2		100.		
60	Nd	.005	.2		50.		
61	Pm						
62	Sm	.00003	.2		100.		
63	Eu	.0000015	.02				
64	Gd	.001	.1		10.		
65	Tb	.0002					
66	Dy	.0000015	.5		10.		
67	Ho	.00002	.2				
68	Er	.001	.5				
69	Tm	.0001	.05				
70	Yb	.0001	.1				
71	Lu	.000015	2.				
72	Hf	.001	0.5				
73	Ta	.00035	1.				



		Methods					
Z	Element	Oak Ridge LITR reactor	Copper spark	Graphite direct- current arc	Flame spectro- photometer	Sensitive color reaction	Ampero- metric titration
74	W	.00015	0.5			0.4	
75	Re	.00003	2.			.05	
76	Os	.001				1.	
77	Ir	.000015	5.			2.	
78	Pt	.005	0.02			0.2	
79	Au	.00015	.2		200.	.1	
80	Hg	.0065	5.	2.	100.	.08	
81	Tl	.03		0.2	1.		
82	Pb	.1	0.05	.2	20.	.03	3.
83	Bi	.02	.2	.2	300.	1.	300.
84	Po						
85	At						
86	Em						
87	Fr						
88	Ra		.1				
89	Ac						
90	Th		.2				
91	Pa		2.				
92	U	.0005	1.		10.	0.7	



## APPENDIX II

### CHART OF NUCLIDES

Appendix II includes the "Chart of Nuclides" printed for the General Electric Company and the accompanying booklet, "Nuclides and Isotopes". The use of the chart is explained very clearly and in some detail in the booklet.



# NUCLIDES and ISOTOPES

BY

JAMES STOKLEY

General Electric Company



Third Edition, 1953

GENERAL  ELECTRIC

*Copyright 1953 by General Electric Company*

# NUCLIDES and ISOTOPES

BY JAMES STOKLEY

GENERAL ELECTRIC COMPANY

Note: This booklet was prepared to accompany the General Electric "Chart of the Nuclides" (revised edition, Dec. 1952). Copies of the chart and booklet may be obtained free by writing Dept. 2-119, General Electric Co., Schenectady 5, N. Y.

WITH modern theories of atomic structure, which depict the atom as a positively charged, dense nucleus, surrounded by one or more electrons, some puzzling facts have been made clearer. For example, the periodic arrangement of the elements can be explained on the basis of the arrangement of the electrons in shells. Those in the outermost shell determine many of the chemical properties of an element, which are similar for a given number in this shell despite the number of inner shells.

More recent studies, however, have been concerned with the nucleus of the atom and from these has come success in the first attempts at the control of so-called "atomic" energy, which is more correctly designated as "nuclear" energy.

What an element shall be is determined by the number of positive electrical charges in the nucleus, which is ordinarily the same as the number of electrons surrounding it. However, an atom can be "ionized" by removing some of these electrons, and though it changes its properties to some extent it remains the same element.

The un-ionized atom is electrically neutral, since the positive charges in the nucleus exactly counteract the negative charges carried by the electrons. Thus, when ionization occurs, with the removal of electrons, the atom is given a positive charge.

In experiments made in 1912 by Sir J. J. Thom-

son, the discoverer of the electron, positive ions of gases were pulled through a narrow tube and fired at a photographic plate. They were deflected by both electrical and magnetic fields working at right angles, so that they were recorded as curved lines. This provided a means of separating different elements, which is used today in a very useful device called the mass spectrometer. Heavier atoms have more inertia and are curved less than those which are lighter and hence more easy to pull from their path.

Not only did Thomson find that different elements produced different curves but, in some cases, it seemed that the same element traced more than one curve. This was the case with the gas neon, for which the accepted chemical atomic weight was 20.2. He found no curve corresponding to this mass, but there were two—a very strong one at mass 20 and a lighter one at mass 22.

From such data it became evident that elements do not, as previously supposed, consist of just one kind of atom. There are actually three kinds of neon atoms. Some 90.9% of the natural element is of mass 20, 8.8% is of mass 22 and 0.26% a third kind, of mass 21. These in combination have an average weight of 20.183, which is given in the chemical tables for neon. Such atoms of the same element but of different mass are called isotopes.

Most elements in the natural state consist of a



mixture of two or more isotopes, though a few, such as beryllium, aluminum, phosphorus and cesium have only one. But even with these, other isotopes are known, which can be produced artificially with high-energy particles from the cyclotron, betatron and other "atom-smashers." Artificial isotopes are mostly radioactive, that is, they spontaneously give off various kinds of rays or particles and decay into other elements.

In addition, there are elements like radium, which are naturally radioactive. These undergo a series of changes and end up as lead. The series beginning with uranium, which includes radium, concludes at lead of mass 206. Another, starting with thorium, comes to an end with lead 208, while a third, known as the actinium series, ends with lead 207. Natural lead is a mixture of all three, as well as of a fourth isotope, of mass 204, giving it an average atomic weight of 207.21. Even before Thomson's discovery of the isotopes of neon, it had been found that lead from sources in conjunction with radioactive ores was different in atomic weight from lead obtained elsewhere, though there had been no good explanation until isotopes were recognized.

Chemists and physicists had long been attracted to the notion that all elements are made up of the same fundamental building blocks, varying by whole numbers. The fact that many elements had actually been determined to have fractional atomic weights introduced some difficulties. The concept of isotopes, however, renewed interest in this idea, and it was recognized that the nucleus of an atom consists of an assemblage of particles called protons, each of which has a mass about 1840 times the mass of an electron. Hydrogen has a nucleus consisting of just one proton, helium has two and lithium three.

However, helium has four times and lithium six times the mass of hydrogen, so at one time it was supposed that there were also electrons in the nucleus. These would neutralize some of the positive charges on the protons and the net charge, which determines the element, would be less. Another proton in a nucleus, along with another electron as well, would not increase the charge but would increase the mass, and so the existence of isotopes of the same element with different mass could be explained.

In 1931 this view was changed when the neutron was discovered. This particle, of the same mass as the proton, has no electrical charge, and is now used to explain the nature of isotopes. Hydrogen consists almost entirely of an atom with a nucleus

that is merely one proton, but there is a small amount (about 0.02%) of "heavy hydrogen," which has a proton and neutron combined in its nucleus. The normal helium nucleus consists of two protons and two neutrons. Lithium, the next in the atomic series, has three protons; but the nucleus of the more common isotope has four neutrons while that of the remaining isotope has only three. As we get into heavier elements, the constitution in general becomes more complex. Mercury, for example, has no less than seven isotopes, of masses 196, 198, 199, 200, 201, 202 and 204. Each one of these, however, has 80 protons, and the difference is in the number of neutrons, which varies from 116 to 124.

Since unlike electrical charges attract and like charges repel, the nucleus of an atom, with all these positive charges so close together, could not exist were it not for other "binding" forces whose nature is still not entirely understood. These are strong enough to overcome the expected electrostatic repulsion and hold the nucleus together. However, with the high-energy particle accelerators, atomic bullets can be produced, such as protons, neutrons, deuterons (nuclei of heavy hydrogen) and alpha particles (nuclei of helium), as well as electrons and x-rays.

Fired into nuclei they produce changes of various kinds. Sometimes they may stick, and produce a heavier nucleus. They may knock out one or more of the particles there and make it lighter. They may temporarily produce a heavier nucleus, which quickly disintegrates into a lighter one. By such means the nuclear physicist runs up and down the table of elements, until to date he has produced many more artificial forms than are known to occur in nature. There are now recognized over 1000 different "nuclides," which is the name given to different kinds of nuclei whether they are of the same or different elements. Of these, 274 are stable forms of natural elements, while the remaining 939 are unstable. Among this number, 53 are nuclides which occur in nature and they are mainly found among the heaviest elements. Since active research in these fields is being conducted in many laboratories, additions and changes in the list are frequently made.

While the masses of the nuclides are approximately whole numbers, accurate work has shown that they may vary from integers by a small amount called the mass defect. The smaller the mass the more tightly bound is the nucleus. The gain in binding energy corresponds to the loss in mass.

# THE CHART OF NUCLIDES

The accompanying chart was originally prepared in the General Electric Research Laboratory, at Schenectady, N. Y., by Dr. G. Friedlander and Dr. M. L. Perlman. The present edition was revised by Dr. John R. Stehn, of the Knolls Atomic Power Laboratory, which is operated by the General Electric Co. for the Atomic Energy Commission. Data available up to Nov. 1, 1952 were used in making the revision.

The general arrangement of the chart is similar to that suggested by Dr. Emilio Segré. Because of its length it is in three sections, which overlap. The numbers along the left-hand side, marking the horizontal rows, give the number of protons in each nucleus, a value designated by  $Z$  and called the atomic number. Each horizontal row thus represents one element, and the spaces that are filled show the known isotopes of that element.

Spaces shaded in gray represent isotopes which occur in nature and are generally considered as stable. Actually, a few of these "stable" nuclides are radioactive but of very long life; these are indicated by black rectangular areas within their spaces. The unshaded spaces represent radioactive isotopes; again, the black rectangular areas in some of them show that they are found on the Earth.

The space at the left end of each row, heavily bordered in black, gives properties of each element as a whole, including the chemical atomic weight according to the 1952 list of the American Chemical Society.

In each of the other occupied spaces there is shown first the chemical symbol (a list of these is given on page 7), followed by the mass number of the nuclide indicated. The mass number, usually designated by  $A$ , is the sum of the number of protons and neutrons in the nucleus. The number of neutrons, therefore, is equal to the difference between the mass number and the atomic number, i.e.,  $A - Z$ . This number is given at the bottom of alternate columns. Thus, each column shows all nuclides having the same number of neutrons.

In analyzing the relative numbers of protons and neutrons, some interesting preferences are displayed. Of the 276 stable nuclides shown on the chart, the following table shows the division between even and odd numbers of each:

PROTONS	NEUTRONS	NUMBER
Even	Even	165
Even	Odd	55
Odd	Even	49
Odd	Odd	5
		<hr/> 274

The significance of these proportions has not yet been fully explained.

It will be noted that lines drawn diagonally over the squares from lower right to upper left connect nuclides which are of different elements, though they have the same mass numbers. For example, calcium 40, with 20 protons and 20 neutrons, has the same mass number as argon 40, which has 18 protons and 22 neutrons. Nuclides of the same mass number are termed isobars.

The data given on the chart are explained at the lower right. For the stable nuclides, after the symbol and mass number, there is given in the second line the percentage of this isotope present in the natural element.

For nuclides that are naturally radioactive, the same information is given in the first line, the second shows the name and abundance, while the third states the half-life, in terms of the units listed under "Time" in the column headed "Symbols." The half-life is the period required for half of the remaining nuclei to disintegrate. The remaining lines show the mode of decay and the radiation emitted (as listed under "Radiation and Decay"), with their energies in millions of electron volts (Mev).

When more than one mode of decay appears, the one that is most prominent appears first (above, or to the left, of the others). Similarly for the radiations emitted.

For nuclides made radioactive artificially similar information (except for abundance) is given, with the addition of a letter before the symbol to show its classification, according to the listing under "Symbols." This gives an idea of the certainty of the identification of the nuclide. In many squares, there appears in the lower right-hand corner a small triangle. This indicates that the nuclide has been found as a product of the fission of uranium 235, induced by slow neutrons.

It will be noted that certain spaces are divided. This occurs when there are two isomeric states, i.e., when there are two nuclides with the same numbers of protons and neutrons. Apparently a difference in arrangement of the particles present causes a difference in the way they decay radioactively.

A radiation appearing in parentheses is one emitted by a short-lived daughter if it is not otherwise clear from the chart that such a radiation is sure to follow the decay of the nuclide in question. For example, 17-day palladium 103 decays by K capture to 56-minute rhodium 103, which then emits a gamma ray or an internal conversion electron corresponding to an isomeric transition of 0.040 Mev. The presence of ( $\gamma$ .040,  $e^-$ ) in parentheses in the Pd-103 square shows that palladium 103 does decay into the unstable isomer of rhodium 103, which then finally decays into the stable rhodium 103. Such radiations in parentheses are generally as characteristic of the nuclide as the radiation it emits during the initial step in its decay.

An important technical datum, shown in a small oval, is the "thermal neutron absorption or activation cross section." This is an index of the ease with which a neutron may enter a nucleus. The larger the cross section, the more readily the neutron is captured. Such cross section may be considered as the area of the region in which a neutron feels the attraction of the nucleus. It is measured in a unit called the "barn," the area of a square a millionth of a millionth of a centimeter on each side. In some cases the cross section is given as the sum of two numbers, representing the values for two possible neutron reactions. These lead to the two alternative nuclides shown as isomers in the next square to the right.

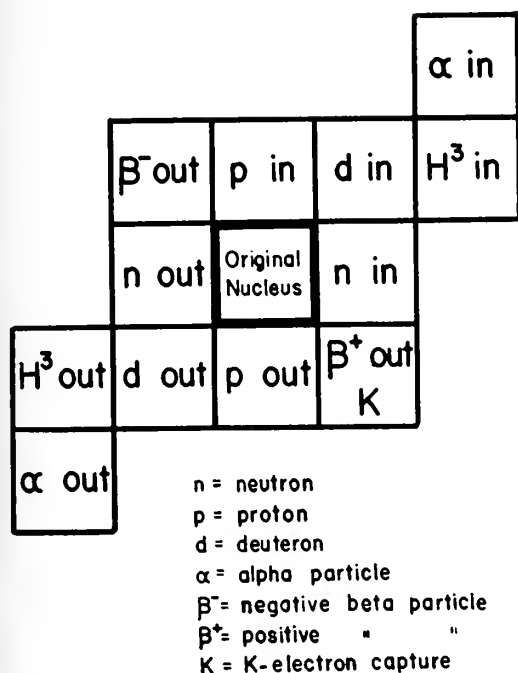


Fig. 1. Relative Locations of the Products of Various Nuclear Processes

There are a few cases wherein the neutron captured causes the nucleus to emit a heavy particle instead of emitting "capture" gamma rays. The cross sections given for He-3 and N-14 are almost entirely for the (n-p) process, wherein a proton is emitted. Those for Li-6 and B-10 are for the (n- $\alpha$ ) process, wherein an alpha particle (He-4 nucleus) is emitted. Cross-sections given for the fissionable nuclides (e.g., U-235 and Pu-239) are solely for the (n- $\gamma$ ), or "capture" process; their cross-sections for fission are not given on the chart.

These cross sections apply only to thermal neutrons, or those moving at the final speed normally attained by a neutron after many collisions. For fast neutrons cross sections are generally smaller.

As nuclear processes occur, whether in natural radioactivity or under conditions induced artificially, the nuclides change, in accordance with the scheme shown in Fig. 1. This involves a kind of nuclear chess game, for each process has its characteristic move. For example, we may follow the natural decay of uranium 238. Reference to the chart shows that an alpha particle is emitted, so the resultant nucleus is in the second space diagonally down to the left. This is uranium  $X_1$ , the same as thorium 234.

It, in turn, emits a negative beta particle (an electron) so there is no loss of mass, but there is a loss of one negative charge, which means that a positive charge is gained. In effect, one neutron has changed into a proton. This move is up and left one space, which brings us to protactinium 234. This has two isomeric states,  $UX_1$  and  $UZ$ , but from each another beta particle is emitted,

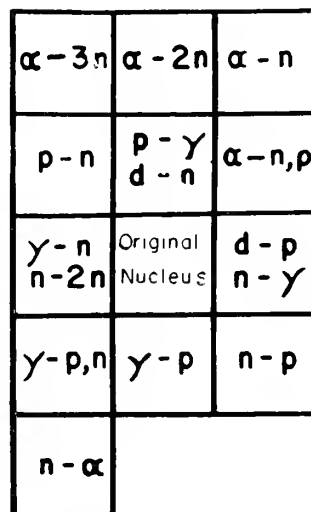


Fig. 2. Changes Produced by Various Nuclear Reactions

which again takes us diagonally upwards to the left, to uranium 234.

Another alpha particle is now emitted, so we shift two spaces diagonally down to the left, to thorium 230, also called ionium. Again an alpha particle comes off, so another shift of the same kind yields radium of mass 226. With yet another alpha particle discharged, the next shift is to emanation 222, which is also called radon.

From this nucleus comes still another alpha particle, so polonium 218—or radium A—is formed. This gives off another alpha particle and lead 214, also called radium B, is next. This is not the end, however, for this kind of lead is unstable, giving off a beta particle to change to radium C, or bismuth 214. With another beta particle off we get to polonium 214, or radium C'. This emits an alpha particle, so again we go downwards diagonally two to the left, arriving at lead 210, radium D.

An alternative route from bismuth 214 to lead 210 is taken in a minute proportion of the disintegrations. In such cases, the bismuth 214 emits an alpha particle to form thallium 210, or radium C'', which then discharges a beta particle and becomes lead 210.

Whichever happens, the lead 210 yields a beta particle, turning into bismuth 210, or radium E. This in turn releases another beta particle, taking us to polonium 210 (radium F). Now comes the final step. An alpha particle is ejected, and there remains lead 206, a stable isotope found in common lead to the extent of 26%. Incidentally, in many of the steps, gamma rays are also emitted.

In the same way, the two other natural radioactive sequences may be traced. One is the actinium series, which starts with uranium 235 and ends with lead 207. The other is the thorium series, which goes from thorium 232 to lead 208. A fourth series is also known, starting with plutonium 241 and ending with bismuth 209.

In Fig. 2 is reproduced a diagram which, like Fig. 1, is shown in the lower right-hand section of the chart. This enables the user to find the effect of various nuclear reactions on a nuclide.

The method commonly used by physicists of representing a nuclear reaction is to give, often in parentheses, the symbol for the particle or radiation hurled at the nucleus, followed by that for the emitted particle (or radiation). These symbols are:

n—neutron	$\alpha$ —alpha particle
d—deuteron	$\gamma$ —gamma ray

Thus a (p- $\gamma$ ) reaction occurs when a proton is the incident particle and a gamma ray is emitted. The charge on the proton increases that of the

nuclide bombarded by one unit, thus raising its atomic number by one and converting it into an isotope of the next higher element. At the same time the mass of the incident proton increases the mass of the nuclide by one, so the net result is a shift to the space immediately above, as indicated in the diagram. Typical of this is the (p- $\gamma$ ) reaction with carbon 12, which converts it to nitrogen 13.

With an (n- $\gamma$ ) reaction, the incident neutron raises the mass by one, but there is no increase in charge or atomic number. Hence the shift is to the next space to the right. An example is that of silver 107, which is converted to silver 108, a short-lived radioactive isotope. An (n-p) reaction produces a shift to the space immediately below and to the right. The neutron adds a unit of mass but the emitted proton takes it away. At the same time the proton removes a unit of charge and thus reduces the atomic number by one, so that it becomes the element on the line below. This occurs with nitrogen 14, which is thereby converted to carbon 14, important in biological studies.

The dashed curved line running diagonally across the chart is the "Line of Beta Stability." Radioactive disintegrations, other than those that emit an alpha particle, tend to go from one isobar to another, without changing the mass number, toward the more stable isobar. If the mass number is odd (e.g., 107), the decay is to the nuclide through which the Line passes (silver 107).

If the mass number is even, the decay is generally (though not always) to the even-even nuclide of that mass number which is nearest to the Line of Beta Stability. For example, silver 106, an odd-odd nucleus, tends to decay to palladium 106, rather than cadmium 106, because palladium 106 is nearer the line, and thus more stable in energy. In the case of silver 108, however, it finds little choice between decaying to palladium 108 or to cadmium 108. The two are about equally far below silver 108 on an energy scale as shown by the fact that the line passes roughly equidistant from the two.

The Line of Beta Stability, in other words, indicates the relative energies of the even-even nuclides of a given mass number and the relative energies of the odd-odd nuclides of a given mass number. It does not tell us how much more stable an even-even nuclide is, compared to an odd-odd nuclide of the same mass number.

The heavy pairs of lines, at  $Z=20, 50$  &  $82$ ; and at  $A-Z=20, 50, 82$  &  $126$ , indicate the so-called "magic numbers." These nuclides contain closed shells of nuclear particles which are particularly tightly bound.

# LIST OF ELEMENTS

ATOMIC NUMBER	SYMBOL	NAME	ATOMIC NUMBER	SYMBOL	NAME
0	n	neutron	49	In	indium
1	H	hydrogen	50	Sn	tin
2	He	helium	51	Sb	antimony
3	Li	lithium	52	Te	tellurium
4	Be	beryllium	53	I	iodine
5	B	boron	54	Xe	xenon
6	C	carbon	55	Cs	cesium
7	N	nitrogen	56	Ba	barium
8	O	oxygen	57	La	lanthanum
9	F	fluorine	58	Ce	cerium
10	Ne	neon	59	Pr	praseodymium
11	Na	sodium	60	Nd	neodymium
12	Mg	magnesium	61	Pm	promethium
13	Al	aluminum	62	Sm	samarium
14	Si	silicon	63	Eu	europium
15	P	phosphorus	64	Gd	gadolinium
16	S	sulfur	65	Tb	terbium
17	Cl	chlorine	66	Dy	dysprosium
18	A	argon	67	Ho	holmium
19	K	potassium	68	Er	erbium
20	Ca	calcium	69	Tm	thulium
21	Sc	scandium	70	Yb	ytterbium
22	Ti	titanium	71	Lu	lutetium
23	V	vanadium	72	Hf	hafnium
24	Cr	chromium	73	Ta	tantalum
25	Mn	manganese	74	W	tungsten
26	Fe	iron	75	Re	rhenium
27	Co	cobalt	76	Os	osmium
28	Ni	nickel	77	Ir	iridium
29	Cu	copper	78	Pt	platinum
30	Zn	zinc	79	Au	gold
31	Ga	gallium	80	Hg	mercury
32	Ge	germanium	81	Tl	thallium
33	As	arsenic	82	Pb	lead
34	Se	selenium	83	Bi	bismuth
35	Br	bromine	84	Po	polonium
36	Kr	krypton	85	At	astatine
37	Rb	rubidium	86	Em	emanation (also called radon, symbol Rn).
38	Sr	strontium	87	Fr	francium
39	Y	yttrium	88	Ra	radium
40	Zr	zirconium	89	Ac	actinium
41	Nb	niobium (formerly columbium, symbol Cb)	90	Th	thorium
42	Mo	molybdenum	91	Pa	protactinium
43	Tc	technetium	92	U	uranium
44	Ru	ruthenium	93	Np	neptunium
45	Rh	rhodium	94	Pu	plutonium
46	Pd	palladium	95	Am	americium
47	Ag	silver	96	Cm	curium
48	Cd	cadmium	97	Bk	berkelium
			98	Cf	californium



*Additional copies of this booklet and the chart it accompanies may be obtained free by writing to Dept. 2-119, General Electric Company, Schenectady 5, N. Y.*



# GENERAL ELECTRIC CHART OF THE NUCLIDES

KNOLLS ATOMIC POWER LABORATORY

(Operated by the General Electric Company for the Atomic Energy Commission)

FOURTH EDITION—REVISED TO NOVEMBER, 1952

## LIST OF ELEMENTS BY CHEMICAL SYMBOL

Al 13	Ge 32	P 15	Te 52
Ar 18	Ga 31	As 33	Tb 65
As 33	Se 34	Ni 28	Ti 22
Br 35	Br 35	Nb 41	Sn 50
C 6	Br 35	Mo 42	U 92
Ca 20	Br 35	Cr 24	V 23
Cd 48	Br 35	Fe 26	W 74
Ce 58	Br 35	Co 27	Xe 54
Cf 98	Br 35	Cu 29	Y 39
Cl 17	Br 35	Dy 64	Yb 70
Cm 96	Br 35	Er 68	Zn 30
Cu 29	Br 35	Fa 88	Zr 40
Dy 64	Br 35	Fr 87	
Er 68	Br 35		
Fa 88	Br 35		
Fr 87	Br 35		

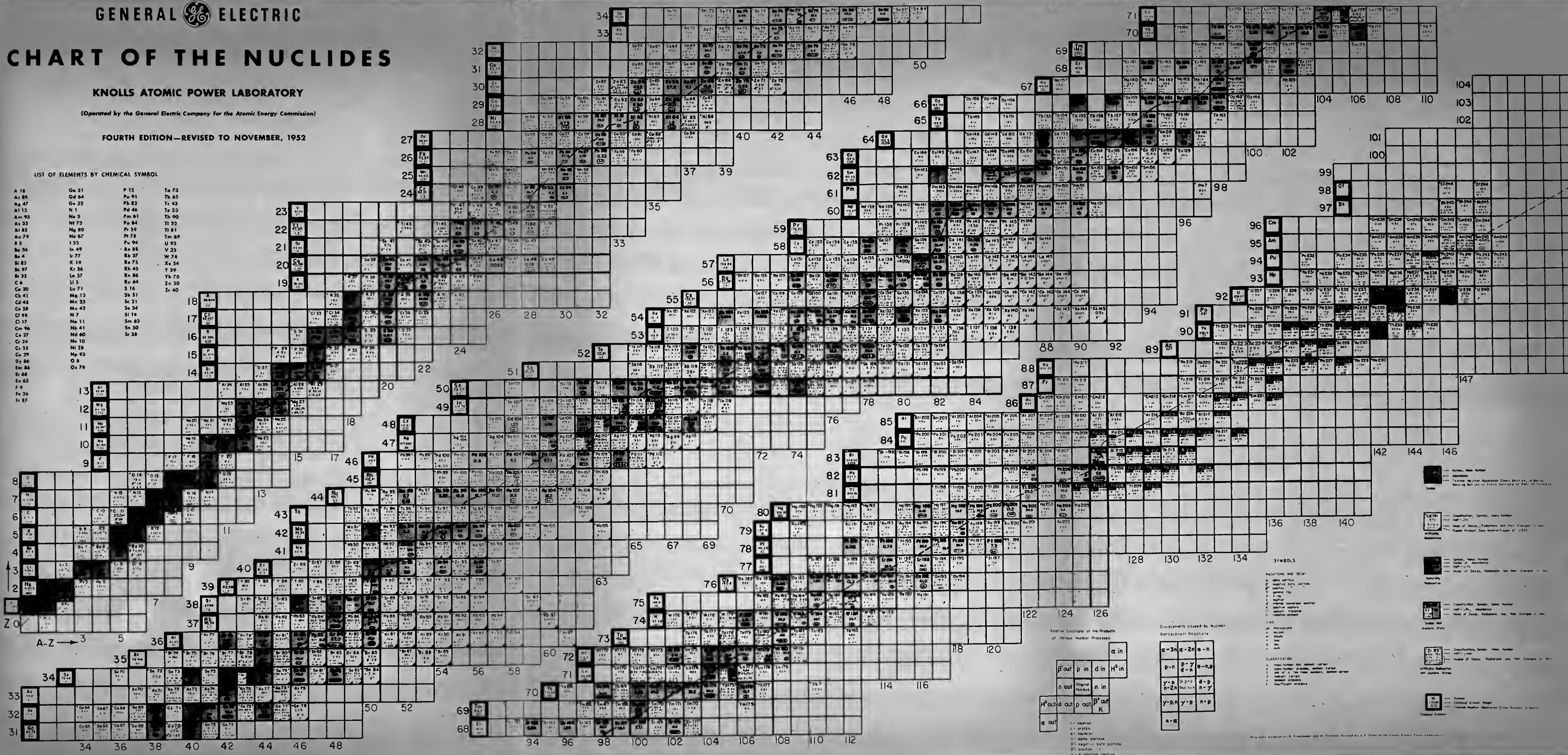


Figure 15.





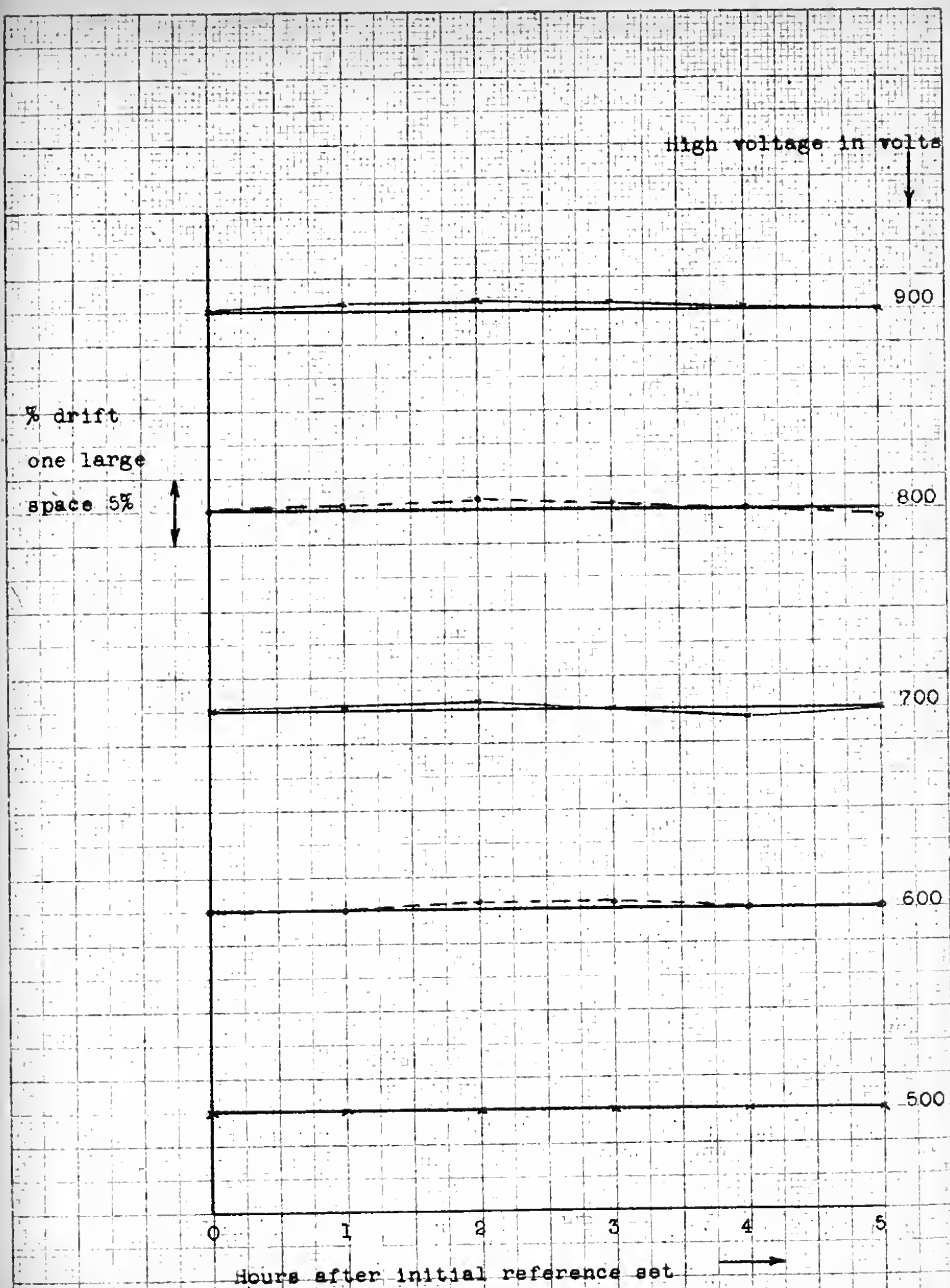


Figure 13.

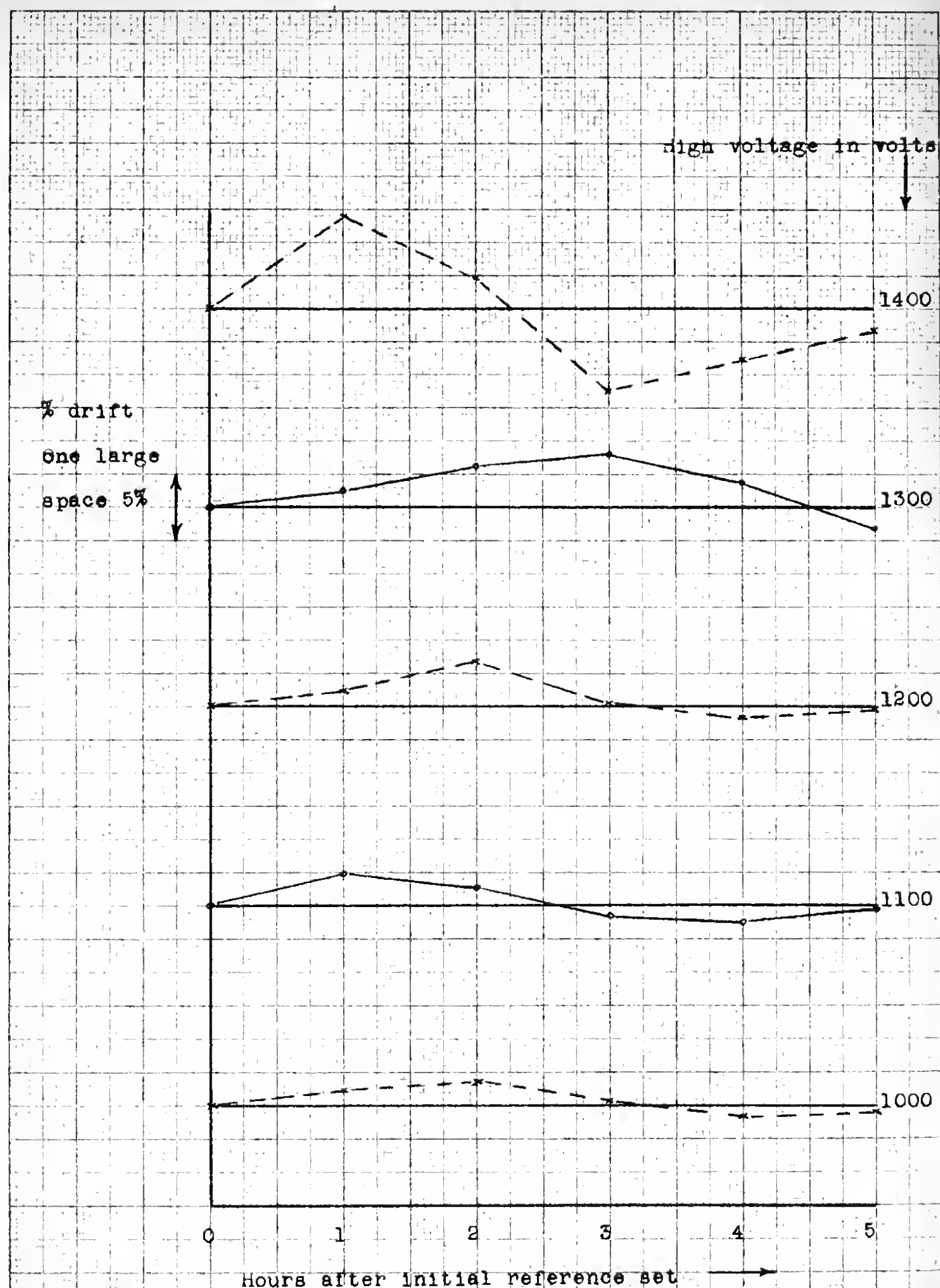


Figure 13.

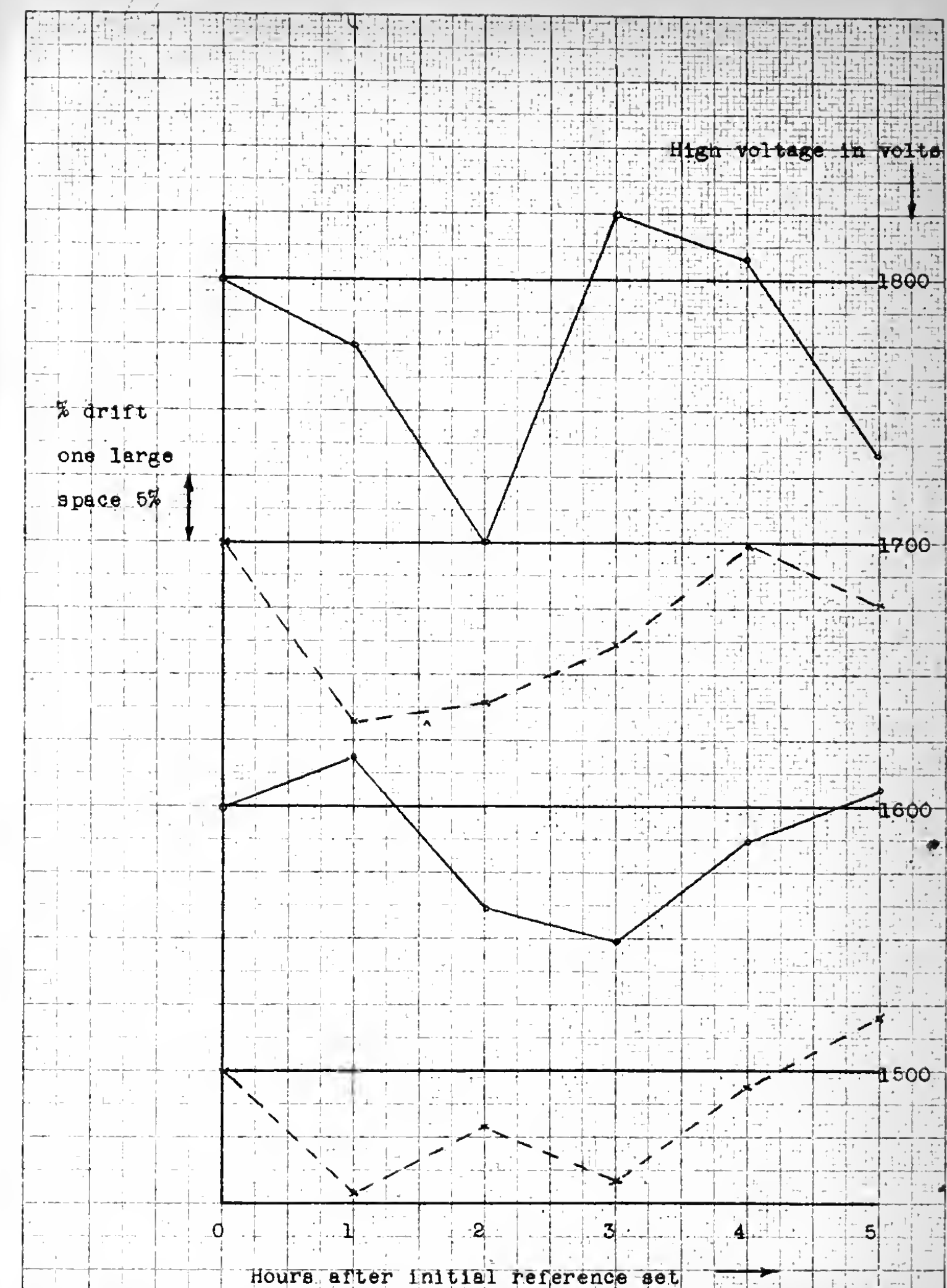


Figure 13.



















OC 14 58  
MY 15 64  
AG 6 64  
28 OCT 65

5382  
12776  
14384  
14806

Thesis

28960

A425

Altekruse

A drift free gamma ray  
spectrometer for neutron  
radioactivation analysis

OC 14 58  
MY 15 64  
AG 6 64  
28 OCT 65

5382  
12776  
14384  
14806

Thesis

28960

A425

Altekruse

A drift free gamma ray  
spectrometer for neutron  
radioactivation analysis.

thesA425

A drift free gamma ray spectrometer for



3 2768 001 89850 5

DUDLEY KNOX LIBRARY